Identification of histone deacetylase genes in *Dendrobium officinale* and their expression profiles under phytohormone and abiotic stress treatments

Mingze Zhang[1,2], Jaime A. Teixeira da Silva[3], Zhenming Yu[1], Haobin Wang[1,2], Can Si[1,2], Conghui Zhao[1,2], Chunmei He[1] and Jun Duan[1]

[1] Key Laboratory of South China Agricultural Plant Molecular Analysis and Gene Improvement, South China Botanical Garden, Chinese Academy of Sciences, Guangzhou, China
[2] College of Life Sciences, University of Chinese Academy of Sciences, Beijing, China
[3] Independent Researcher, Miki, Kagawa, Japan

ABSTRACT

The deacetylation of core histones controlled by the action of histone deacetylases (HDACs) plays an important role in the epigenetic regulation of plant gene transcription. However, no systematic analysis of *HDAC* genes in *Dendrobium officinale*, a medicinal orchid, has been performed. In the current study, a total of 14 histone deacetylases in *D. officinale* were identified and characterized using bioinformatics-based methods. These genes were classified into RPD3/HDA1, SIR2, and HD2 subfamilies. Most *DoHDAC* genes in the same subfamily shared similar structures, and their encoded proteins contained similar motifs, suggesting that the *HDAC* family members are highly conserved and might have similar functions. Different *cis*-acting elements in promoters were related to abiotic stresses and exogenous plant hormones. A transient expression assay in onion epidermal cells by *Agrobacterium*-mediated transformation indicated that all of the detected histone deacetylases such as DoHDA7, DoHDA9, DoHDA10, DoHDT3, DoHDT4, DoSRT1 and DoSRT2, were localized in the nucleus. A tissue-specific analysis based on RNA-seq suggested that *DoHDAC* genes play a role in growth and development in *D. officinale*. The expression profiles of selected *DoHDAC* genes under abiotic stresses and plant hormone treatments were analyzed by qRT-PCR. *DoHDA3*, *DoHDA8*, *DoHDA10* and *DoHDT4* were modulated by multiple abiotic stresses and phytohormones, indicating that these genes were involved in abiotic stress response and phytohormone signaling pathways. These results provide valuable information for molecular studies to further elucidate the function of *DoHDAC* genes.

Subjects Agricultural Science, Bioinformatics
Keywords *Dendrobium officinale*, Histone deacetylation, Phylogenetic analysis, Subcellular localization, Stress

INTRODUCTION

Higher plants have a sessile lifestyle and often suffer from exposure to abiotic stresses such as drought, cold or high salinity (*Shao, Wang & Tang, 2015*). Various stress-inducing genes and signaling factors with different functions participate in stress responses, and the expression of these genes usually depends on chromatin remodeling (*Kim et al., 2010*).

The eukaryotic genome is stored in a nuclear protein complex composed of nucleosomes (*Teif & Clarkson, 2019*). In the nucleosome, two copies of histone H2A, H2B, H3, and H4 form a histone octamer, which is surrounded by DNA 147 base pairs long (*Luger et al., 1997*). The basic residues such as lysine and arginine in the N-terminal tail of each histone are covalently modified by acetylation to regulate the transcription of genes wrapped around the core histone (*Srivastava, Singh & Dubey, 2016*). Since a report that indicated that gene activity is related to histone acetylation, the modification of histone acetylation and deacetylation have received increasing attention (*Grunstein, 1997*). Generally, the acetylation of lysine residues in H3 and H4 N-tails neutralizes the positive charge of the histone tails, thereby reducing their affinity for DNA strands, hence histone acetylation mediated by histone acetyltransferases (HATs), which connect acetyl groups to histones, promotes loosening of the chromatin structure and activates gene transcription (*Berger, 2007*; *Kim et al., 2015*; *Shahbazian & Grunstein, 2007*). Conversely, histone deacetylation mediated by histone deacetylases (HDACs), which remove an acetyl group from histones, facilitates the formation of compact chromatin leading to the repression or silencing of genes (*Hollender & Liu, 2008*).

HDACs are widespread in eukaryotes from yeast to mammals and plants, and the mechanism by which histone modification leads to the repression of gene expression is conserved (*Kim et al., 2015*). For example, in *Arabidopsis thaliana*, histone acetylation modification sites were identified by mass-spectrometry and biochemical assays, and were shown to be highly conserved in other eukaryotes (*Kim et al., 2015*). Based on sequence homology with yeast HDACs, plant HDACs are classified into three different groups, including Reduced Potassium Dependency-3/Histone Deacetylase 1 (RPD3/HDA1), which requires a zinc ion cofactor for deacetylase activity (*Yang & Seto, 2007*), Silent Information Regulator 2 (SIR2), which depends on nicotinamide adenine dinucleotide (NAD^+), and Histone Deacetylase 2 (HD2), which is unique in plants (*Hirschey, 2011*; *Pandey et al., 2002*). Researchers have identified and characterized some *HDAC* genes in a wide range of plant species, such as maize (*Zea mays*) (*Forestan et al., 2018*), *A. thaliana* (*Hollender & Liu, 2008*), rice (*Oryza sativa*) (*Fu, Wu & Duan, 2007*), barley (*Hordeum vulgare*) (*Demetriou et al., 2009*), potato (*Solanum chacoense*) (*Lagacé et al., 2003*), grape (*Vitis vinifera*) (*Busconi et al., 2009*), tobacco (*Nicotiana tabacum*) (*Bourque et al., 2011*), black cottonwood (*Populus trichocarpa*) (*Alinsug, Yu & Wu, 2009*), banana (*Musa acuminata*) (*Fu et al., 2018*), soybean (*Glycine max*) (*Yang et al., 2018*), litchi (*Litchi chinensis*) (*Peng et al., 2017*), common bean (*Phaseolus vulgaris*) (*Hayford et al., 2017*), common liverwort (*Marchantia polymorpha*) (*Chu & Chen, 2018*) and tomato (*Solanum lycopersicum*) (*Zhao et al., 2015*), and have studied the functions of certain *HDAC* genes. For example, *HDAC* genes are involved in plant responses to stress-related hormones such as salicylic acid (SA), abscisic acid (ABA) or jasmonic acid (JA) and stress stimuli such as drought, cold, salt, and pathogens (*Ma et al., 2013*). *AtHDA6* and *AtHDA19* regulate gene expression induced by ABA and salt stress in *A. thaliana* (*Chen & Wu, 2010*). Overexpression of *AtHD2C* made transgenic *A. thaliana* plants insensitive to ABA and tolerant to salt and drought stresses (*Sridha & Wu, 2006*). However, the molecular functions of many of these HDAC proteins, which are histone modifiers, have not yet been well characterized.

Dendrobium Swartz is the second largest genus of the Orchidaceae, which consists of nearly 1,600 accepted species (*Juswara, Schuiteman & Champion, 2019*). Among them, *Dendrobium officinale* Kimura et Migo is a popular tonic and traditional Chinese medicine (TCM) with high commercial value, containing compounds with antioxidant and antitumor activity (*Li et al., 2011*; *Teixeira da Silva & Ng, 2017*; *Wu et al., 2014*). In addition to polysaccharides thought to be among the major active ingredients of *D. officinale*, a wide variety of low molecular weight compounds including bibenzyls, phenanthrenes, and flavanones have been detected by phytochemical analyses (*Chen et al., 2012*). *D. officinale* grows well under a suitable environment (*Ding et al., 2018*; *Yang et al., 2014*). In a natural environment, *D. officinale* is in an epiphytic state, often growing on humid rocks in mountain climates at an altitude of 500–1600 m, or on the tree trunks in virgin forests with warm and moist environments (*Zeng et al., 2019*). Based on its growth habits, *D. officinale* is susceptible to abiotic stresses such as high and low temperatures, drought and salinization, resulting in low natural reproduction rate and slow growth (*Zeng et al., 2019*).

Phytohormones not only mediate developmental processes in plants but can also sustainably alleviate adverse effects of abiotic and biotic stresses in plants (*Wolters & Jurgens, 2009*). For instance, SA improved plant abiotic stress tolerance via SA-mediated control of major plant metabolic processes by strengthening salinity and drought stress tolerance (*Khan et al., 2015*). The JA signaling pathway plays a key role in coordinating the activation of biosynthetic routes involved in defense-related metabolites (*Ballare & Austin, 2019*). Secondary metabolites, including terpenes, phenolics, compounds with nitrogen, and others, which are biosynthetically derived from primary metabolites, have also been established as beneficial for plants' tolerance to biotic and abiotic stresses (*Ramakrishna & Ravishankar, 2011*). Environmental stresses trigger the biosynthesis of certain secondary metabolites in plants which are important candidates for human nutrition (*Ashraf et al., 2018*). Furthermore, epigenetic regulation of gene expression is important for a plant's adaptation to environmental changes (*Zheng et al., 2020*). Therefore, understanding how histone acetylation modification is involved in the responses of *D. officinale* to environmental stresses will contribute significantly to our understanding of the molecular mechanisms underlying epigenetic regulation in this orchid. However, studies on the evolutionary relationships and functional characteristics of *HDAC* genes in *D. officinale* (*DoHDAC* genes) are scarce.

The genome and transcriptome sequences of *D. officinale* are now available, allowing the *DoHDAC* genes to be isolated and identified (*Shen et al., 2017*). In this study, fourteen *DoHDAC* genes were identified from the *D. officinale* genome and their structure, phylogeny, conserved motifs, and putative promoter were analyzed. Subsequently, the subcellular localization and expression patterns of selected *DoHDAC* genes under hormone, salt, drought and cold treatments were analyzed. These results provide a foundation for further clarifying the functions of DoHDAC proteins.

MATERIAL AND METHODS

Identification and bioinformatics analysis of *DoHDAC* genes

To identify potential *DoHDAC* genes, the coding sequences (CDSs) of *AtHDAC* genes were used for a BLASTP algorithm-based query against the *D. officinale* genome database (https://www.ncbi.nlm.nih.gov/genome/?term=Dendrobium, NCBI Biosample ID: SAMN03083363). Genes were identified by a hidden Markov model search based on the HDAC domain using the Pfam protein domain database. To determine the sequence identity among HDACs, full-length amino acid sequences of HDAC proteins were aligned and compared using *DNAMAN 8* software (Lynnon Biosoft, San Ramon, CA, USA). For phylogenetic analysis, the amino acid sequences of HDAC proteins from *D. officinale*, *A. thaliana* and *O. sativa* in *FASTA* format were aligned with Clustal X 2.0 (*Larkin et al., 2007*), and sequence identity was calculated by UniProt BLAST (http://www.uniprot.org/blast/), and then a neighbor-joining phylogenetic tree was constructed using the *MEGA 7* program (*Kumar, Stecher & Tamura, 2016*) with a bootstrap analysis of 1000 replicates. Nucleus localization signals (NLSs) were found in amino acid sequences of DoHDAC proteins at http://localizer.csiro.au/ (*Sperschneider et al., 2017*). Recognizable conserved domains of DoHDAC proteins were identified with EBL-EBI (http://www.ebi.ac.uk/interpro/search/sequence-search) and also verified by the CDD database (https://www.ncbi.nlm.nih.gov/cdd). The domain architecture was drawn using DOG2.0 software (*Ren et al., 2009*). The protein sequence motifs of DoHDAC proteins were identified using MEME (http://memesuite.org/tools/meme) (*Bailey et al., 2009*). Gene structure analysis of the *DoHDAC* genes was conducted with GSDS (Gene Structure Display Server, http://gsds.gao-lab.org/) (*Hu et al., 2014*). The functional interacting networks of functional proteins were integrated in STRING (https://string-db.org/) based on an *A. thaliana* association model with the confidence parameter set at a threshold of 0.700 and no more than 20 interactors (*Szklarczyk et al., 2019*). DNA sequences about 2000 bp long upstream of the initiation codon ATG of *DoHDAC* genes were regarded as putative promoters. *Cis*-elements in these promoters were analyzed using the online program PlantCare (http://bioinformatics.psb.ugent.be/webtools/plantcare/html/). The predicted *cis*-acting elements of promoters of *DoHDAC* genes were illustrated by TBtools software (*Chen et al., 2020*).

Subcellular localization assays

The CDSs of *DoHDA7*, *DoHDA9*, *DoHDA10*, *DoHDT3*, *DoHDT4*, *DoSRT1* and *DoSRT2* without a termination codon were cloned into binary vector pCAMBIA1302 with the green fluorescent protein (GFP) (GenBank Accession No. AF234298) with the *Nco* I restriction enzyme. The resulting binary vectors, pCAMBIA1302-*DoHDA7*, pCAMBIA1302-*DoHDA9*, pCAMBIA1302-*DoHDA10*, pCAMBIA1302-*DoHDT3*, pCAMBIA1302-*DoHDT4*, pCAMBIA1302-*DoSRT1* and pCAMBIA1302-*DoSRT2*, were transferred into *Agrobacterium tumefaciens* strain EHA105 (Shanghai Weidi Biotechnology Co. Ltd., Shanghai, China), according to the manufacturer's protocol. Then, using *Agrobacterium*-mediated transformation, these recombinant binary vectors were transformed into epidermal cells of onion (*Allium cepa* L. "Red Sun") (*Huang et al., 2011*). A Zeiss Model

Axio Imager A2 upright fluorescence microscope (Carl Zeiss, Oberkochen, Germany) was used to observe gene expression in transformed onion epidermal cells. In order to show the nucleus, according to the manufacturer's protocol, the epidermal cell layers were stained with 2-(4-amiylphenyl)-6-indolecarbamoyl dihydrochloride (DAPI) staining solution (Beyotime Biotech Inc., Shanghai, China). The positive control was onion epidermal cells with an empty pCAMBIA1302-GFP vector. ZEN 2011 software (Carl Zeiss) was used to analyze cellular localization.

Plant materials and treatments

Based on previously reported concentrations (*He et al., 2017*), *D. officinale* plantlets with a stem length of about three cm growing on half-strength Murashige and Skoog (MS; (*Murashige & Skoog, 1962*) (1/2 MS) agar medium containing 2% sucrose were separately exposed to one of several abiotic stresses: 100 μM gibberellic acid (GA$_3$), 100 μM ABA, 100 μM SA, 200 μM methyl jasmonate (MeJA), 15% polyethylene glycol (PEG)-6000 (all compounds: Sigma-Aldrich, Shanghai, China), 250 mM NaCl (Guangzhou Chemical Reagent Factory, Guangzhou, China) and 4 °C , separately. Five *D. officinale* plantlets were used for each treatment. Plant tissues, including roots, stems and leaves, were harvested at different selected time points after applying the above treatments, then immediately frozen in liquid nitrogen for further gene expression experiments. Based on the transcriptome data, the expression patterns of *DoHDAC* genes in different tissues were analyzed, and a heatmap was generated with the heatmap software package on the BMKCloud platform (http://www.biocloud.net).

About 100 mg of samples, including leaves, roots and stems from previously collected *D. officinale* plants, were placed in a pre-chilled mortar and ground with liquid nitrogen to a fine powder. Each finely powdered sample was transferred to a 2 mL microcentrifuge tube containing 1.5 mL of pre-warmed extraction buffer (50 mM Tris–HCl, 20 mM EDTA, 1 M NaCl, 2% SDS and 4% β-mercaptoethanol; pH 8.0). Samples were incubated in a water bath at 65 °C for 15–20 min. The tube was centrifuged at 13,000 g for 10 min at 4 °C and the supernatant was transferred to a sterile 2 mL centrifuge tube. An equal volume of water-saturated phenol (pH 4.5) was added, vortexed for 2 min, then kept at room temperature for 10 min. The tube was centrifuged at 13,000 g for 10 min at 4 ° C, the supernatant was transferred to a sterile 2 mL centrifuge tube, then equal volumes of chloroform and isoamyl alcohol (24/1, v/v) were added and mixed thoroughly. The tube was again centrifuged at 13,000 g for 10 min at 4 °C, the supernatant was transferred to a sterile two mL centrifuge tube, and an equal volume of isopropanol was added. The solution in the centrifuge tube was mixed, placed in a refrigerator at −20 °C for 10 min, and then centrifuged at 13,000 g for 10 min at 4 °C. The supernatant was discarded, the pellet was washed with 75% chilled ethanol, and the tube was centrifuged at 13,000 g for 15 min at 4 °C. The RNA pellet was dried at room temperature for 5 min. The dried RNA pellet was resuspended in 50 μL of diethyl phosphorocyanidate (DEPC) in distilled water. According to the manufacturer's instructions, samples were treated with Recombinant DNase I (RNase-free) (Takara Bio Inc., Kusatsu, Shiga, Japan) to remove genomic DNA, and stored at −80 °C. The NanoDrop One/OneC micro nucleic acid protein concentration

analyzer (Thermo Fisher Scientific, Waltham, MA, USA) was used to assess the purity and concentration of RNA samples. Agarose gel electrophoresis was used to survey the RNA integrity by Clinx GenoSens gel documentation system (Clinx Science Instruments, Shanghai, China).

Quantitative real-time reverse transcriptase-PCR analysis

Following the manufacturer's instructions, the first-strand cDNA was synthesized using the GoScript[TM] Reverse Transcription System (Promega, Madison, WI, USA). Quantitative real-time reverse transcriptase-PCR (qRT-PCR) assays of three biological replicate samples were performed on a LightCycler 480 system (Roche, Basel, Switzerland) using the Aptamer[TM] qPCR SYBR® Green Master Mix (Tianjin Novogene Bioinformatics Technology Co. Ltd., Tianjin, China). The reaction conditions were as follows: 95 °C for 5 min, followed by 40 cycles of 95 °C for 10 s, and 60 °C for 30 s. *D. officinale* actin (NCBI accession number JX294908) was used as an internal control gene based on the advice of *He et al. (2015)*. The relative expression levels of genes were calculated using the $2^{-\Delta\Delta CT}$ method (*Livak & Schmittgen, 2001*). The expression of genes was significantly altered upon different treatments when the fold change was greater than 2 (*Li et al., 2016*). The gene-specific primers for qRT-PCR were designed by Primerquest (https://sg.idtdna.com/Primerquest/Home/Index) and are listed in Table S1.

RESULTS

Identification and phylogenetic analysis of the *DoHDAC* genes

In this study, 14 *DoHDAC* genes were identified in the *D. officinale* genome. The CDS length of *DoHDAC* genes was diverse, ranging from 267 bp to 2085 bp (Table 1). Analysis of gene structure helps to understand gene function and evolution (*Feng et al., 2016*). Hence, the structure of the *DoHDAC* genes was analyzed. Our results showed that their conserved coding regions consisted of different numbers of exons, while *DoHDA10* and *DoHDT4* have only one exon (Fig. 1). Amino acid sequence alignment of the 14 DoHDAC proteins showed that, except for DoHDA4 and DoHDA10, the eight histone deacetylases with amino acid sequences between 200 aa and 312 aa all contained a typical histone deacetylase catalytic domain. DoHDA4 and DoHDA10 showed significantly low sequence identity with other RPD3/HDA1 family proteins in *D. officinale* (Fig. 2), suggesting that they might play some unique roles in certain cellular events. Functional domain analysis revealed that DoHDA6 possessed a RanBP2-type zinc finger domain (Fig. 2). DoHDT3 contained a conserved domain with a pentapeptide (MEFWG) on the N-terminus and a C_2H_2 zinc finger domain on the C-terminus of the protein (Fig. S1, Fig. 2). In addition, DoSRT1 and DoSRT2 possessed a single copy of the sirtuin-type HDAC domain (Fig. 2). To investigate the conserved nature of motifs in DoHDAC proteins, we investigated 10 motifs among the 14 DoHDAC proteins. The width of these 10 motifs ranged from 21 (motif 6, 8 and 9) to 50 (motif 3, 4 and 5) amino acids (Fig. 3). Closely related proteins, such as DoHDA3, DoHDA7, DoHDA9, DoHDA1, DoHDA6, DoHDA2, DoHDA5, DoHDT3 and DoHDT4, had similar conserved motifs. For instance, most of the *D. officinale* RPD3/HDA1 superfamily proteins contained HDACs domain motifs 1 and 2. However, the HDAC

Gene	CDS length (bp)	Protein attributes		
		Length (aa)	MW (Da)[*]	pI[*]
DoHDA1	945	314	34352.98	6.49
DoHDA2	2058	685	76108.86	5.06
DoHDA3	1269	422	105199.42	5.06
DoHDA4	432	143	15457.30	5.69
DoHDA5	1149	382	41545.88	5.44
DoHDA6	1695	564	62307.71	6.31
DoHDA7	1536	511	57896.33	5.30
DoHDA8	816	271	30616.14	6.25
DoHDA9	1500	499	55436.99	5.45
DoHDA10	456	151	16728.54	6.27
DoHDT3	960	319	76918.49	5.15
DoHDT4	267	88	10000.50	6.25
DoSRT1	1230	409	45501.65	8.19
DoSRS2	840	279	30821.09	7.04

Notes.

[*]The theoretical isoelectric point (pI) and molecular weight (Mw) of the *D. officinale* HDAC proteins were calculated with the Compute pI/Mw online tool (https://web.expasy.org/compute_pi/).

domain motif was not found in DoSRT1 and DoSRT2. We constructed a protein–protein interaction network of the 14 DoHDAC proteins using STRING (http://string-db.org/) based on an *A. thaliana* association model (Fig. 4). DoHDA9 showed a high degree of amino acid sequence similarity to AtHDA6, thus it might interact with the flavin-containing amine oxidoreductase family protein (FLD), which might be histone demethylase that promotes flowering by repressing FLOWERING LOCUS C (FLC) (Table S3, Fig. 4, Table S4). Moreover, DoHDA9 might interact with the WD40 repeat-containing protein HOS15 in response to abiotic stress (Table S4). To study the evolutionary relationships among DoHDAC proteins, a phylogenetic tree was constructed by aligning the amino acid sequences of histone deacetylases of four, ten and one HDAC proteins from *A. thaliana*, *O. sativa*, and *Z. mays* using MEGA 7.0. In the phylogenetic tree, 14 DoHDAC proteins were divided into three families: RPD3/HDA1, SIR2, and HD2 (Fig. 5). DoHDA9, AtHDA6 homologue, shared approximately 71.1% amino acid sequence similarity with AtHDA6. In addition, DoHDA7, AtHDA19 homologue, had approximately 80% amino acid sequence similarity with AtHDA19.

Subcellular localization analysis of selected *DoHDAC* genes

To verify the subcellular localization of certain DoHDAC proteins, an *Agrobacterium*-mediated transient transformation system was used in onion epidermal cells. The expression of *GFP* fused to *DoHDA7*, *DoHDA9*, *DoHDA10*, *DoHDT3*, *DoHDT4*, *DoSRT1* and *DoSRT2* was tracked by the GFP marker signal. The blue fluorescence pattern of DAPI-stained cells completely merged with the green fluorescence pattern, showing the nuclear localization of DoHDAC proteins in onion epidermal cells (Fig. 6). As shown in Fig. 6, the positive control
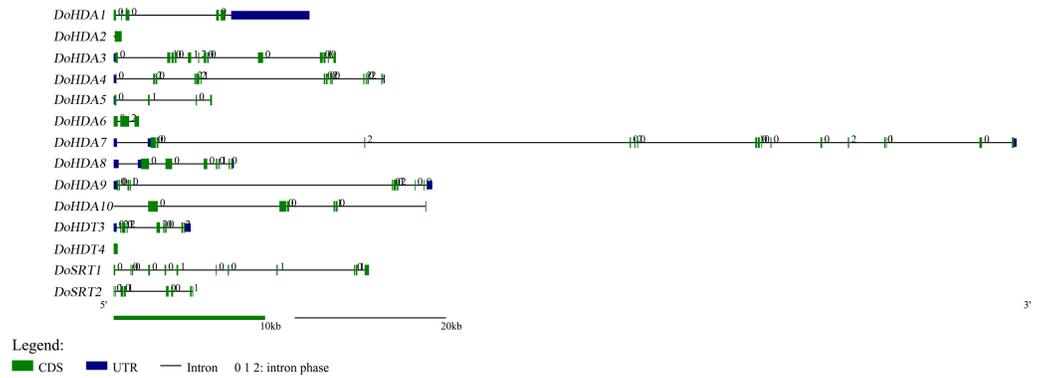
Figure 1 Exon-intron structures of *DoHDAC* genes. Untranslated regions, exons and introns are indicated by blue, green and black, respectively. The green scale bar represents 10 kb. The black scale line represents 20 kb.
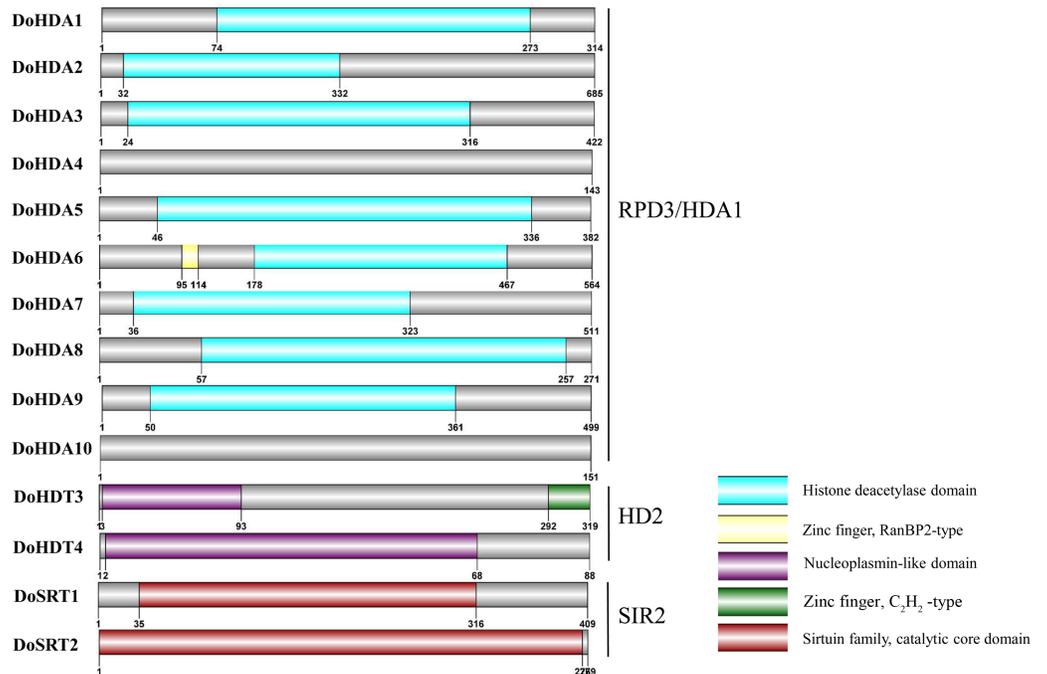
Figure 2 Conserved domain of *DoHDAC* genes. The location and size of domains are shown by different colors. Proteins belonging to each family are grouped together.

was distributed throughout the onion cells. In contrast, DoHDA7, DoHDA9, DoHDA10, DoHDT3, DoHDT4, DoSRT1 and DoSRT2 were localized in the nucleus.

Analysis of *cis*-acting elements in the putative promoters of *DoHDAC* genes

A *cis*-acting element is a non-coding part of DNA, is usually limited to the 5′ upstream region of a gene, and is responsible for transcriptional regulation. To better predict gene

Motif Symbol Motif Consensus
1. RVLIIDIDVHHGBGTEEAFYTTDRVLTVSFHKYGDYF
2. HHAKKCEASGFCYFNBIALAILYLLKYH
3. LPGGIGDESYVYLFKPIIAPVAEEFKPDIIILQAGADSLAGDPLGGFNLT
4. YTIRNVARCWCYETAVALGVELDNKJPYNEYYEYFGPDYTLHIQPKNMEN
5. RRVAYFYDPDVGNYYYGQGHPMKPHRIRMTHNLVVHYGLHQKMEVYRPHP
6. GTGDIKEIGEGKGKGYSLNIP
7. QGEDCLVFEGGYNLCSLSASVSATAKVLL
8. DJARFHAEDYVEFLESITPET
9. GHAECVRFLRSFNVPLLVLGG
10. KNSRQDLEDIRNKLLENLSRLRHAPSVPFQERPPDTEFPEPEEVDDDP

Name | p-value | Motif Locations | Motif Logo

DoHDA1 | 1.59e-96
DoHDA2 | 9.58e-103
DoHDA3 | 3.36e-246
DoHDA4 | 1.73e-8
DoHDA5 | 1.98e-86
DoHDA6 | 4.04e-98
DoHDA7 | 0.00e+0
DoHDA8 | 4.12e-33
DoHDA9 | 0.00e+0
DoHDA10 | 2.67e-12
DoHDT3 | 5.21e-12
DoHDT4 | 1.55e-11
DoSRT1 | 2.05e-1
DoSRT2 | 6.29e-2

Figure 3 Conserved motifs analysis of the DoHDAC proteins. The conserved protein sequence motifs of the DoHDAC proteins were identified using the MEME program. Each motif is represented by a different color.

Full-size DOI: 10.7717/peerj.10482/fig-3

functions, we identified the *cis*-acting elements within the putative ~2 kb promoter region of *DoHDAC* genes. In addition to the core *cis*-acting elements, such as the TATA-box and the CAAT-box, several other *cis*-elements related to plant growth or development, stress responses, and hormone responses were detected (Table S2, Fig. 7). *Cis*-acting elements related to growth or development included light-responsive elements such as Box4, G-box, GT1-motif, Sp1, and TCT-motif, elements expressed only in the endosperm such as the AACA_motif and GCN4_motif, and elements under circadian control or showing meristem-specific activation such as CAT-box and NON-box. *Cis*-acting elements related to phytohormone responses included GA-responsive elements such as GARE-motif, P-box and TATC-box, MeJA-responsive elements such as CGTCA-motif and TGACG-motif, ABA-responsive element (ABRE), and SA-responsive element such as TCA-element. *Cis*-acting elements related to abiotic stresses included drought-responsive elements such as MBS and a low-temperature-responsive (LTR) element. For example, both *DoHDA3* and *DoHDT3* had *cis*-acting elements involved in MeJA-responsiveness, low-temperature responsiveness and drought inducibility. Therefore, based on the large number of *cis*-acting elements related to these stresses, the *D. officinale* plantlets were treated with SA, MeJA, ABA, GA_3, cold stress and drought stress.
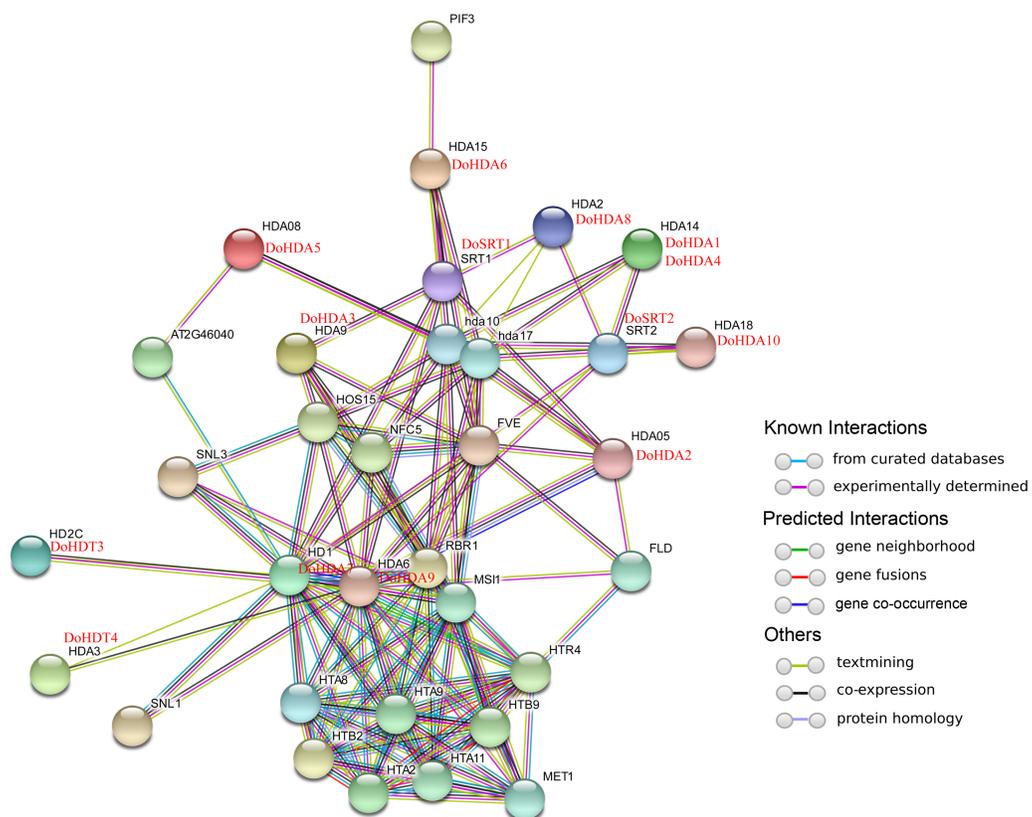
Figure 4 **Interaction networks of DoHDAC proteins according to the orthologs in *A. thaliana*.** Different colored lines represent types of evidence for the association.

Full-size ▣ DOI: 10.7717/peerj.10482/fig-4

Expression analysis of *DoHDAC* genes in different tissues

Since high-throughput sequencing has been performed on *D. officinale* tissues at different developmental stages, the publicly available RNA-seq data obtained is a useful resource for studying gene expression profiles. We used previously reported transcriptome data (*Zhang et al., 2017*) to examine the expression pattern of *DoHDAC* genes in different tissues. The heat map (Fig. 8) revealed that three *DoHDAC* genes (*DoHDA3*, *DoHDA7*, and *DoHDT3*) were highly expressed with FPKM values > 25 in all detected tissues, while *DoHDA10* showed a low expression with FPKM values < 5 in all the detected tissues. In addition, some genes displayed a tissue-specific expression pattern. For example, *DoHDA5* and *DoSRT1* were most highly expressed in the white parts of root, while *DoHDA6* and *DoHDT4* were expressed predominantly in flower buds (Fig. 8). These results suggested that *DoHDAC* genes might play an important role in the development of different organs.

Expression analysis of *DoHDAC* genes in response to exogenous phytohormones

Hormones play a vital role in the vegetative and reproductive growth of plants. Analysis of the *cis*-acting elements in promoters indicates that the *DoHDAC* genes might respond to a variety of stresses and signaling molecules. Therefore, based on potential *cis*-acting
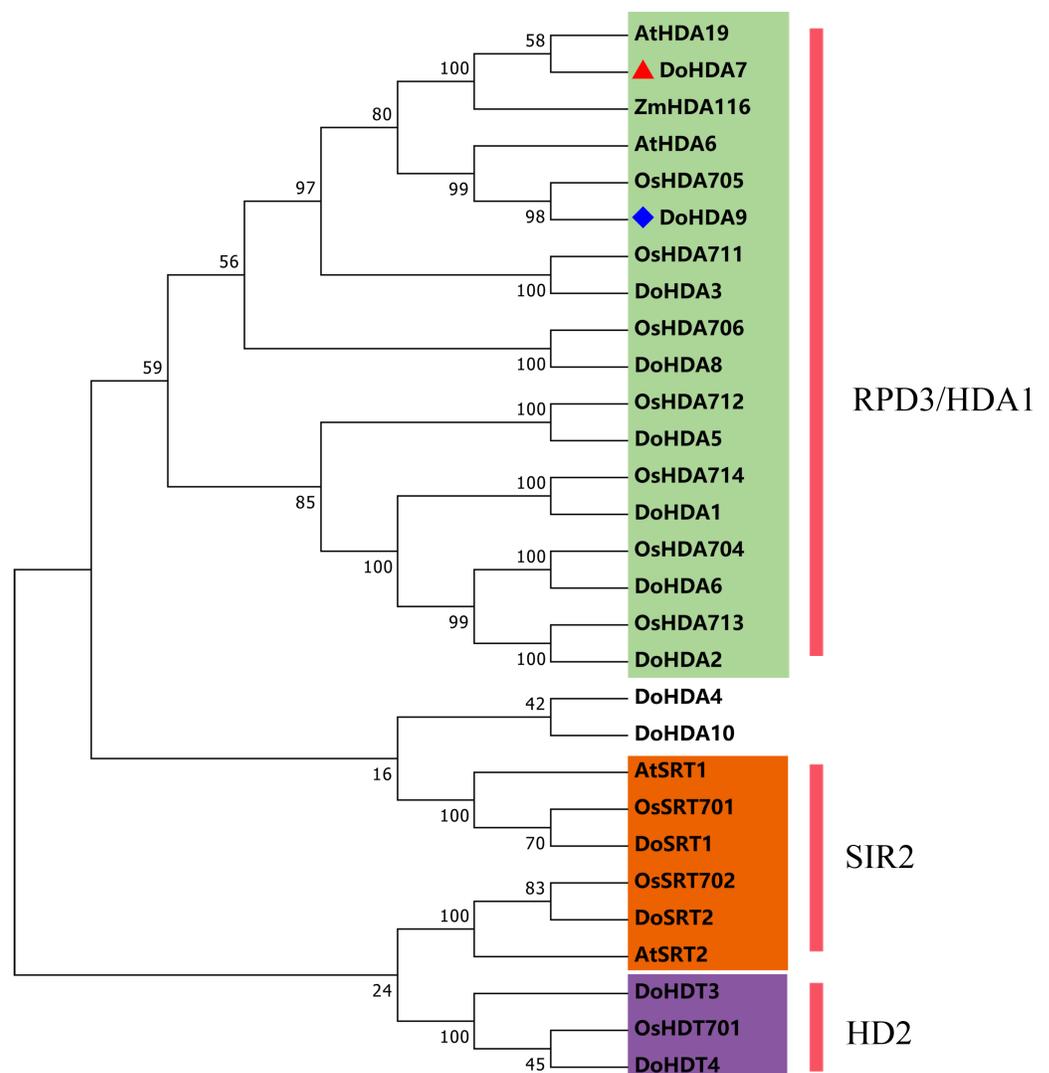
Figure 5 Phylogenetic tree of the deduced amino acid sequences of HDAC proteins in *D . officinale*, *O. sativa*, *A. thaliana*, and *Z. mays.* Abbreviations for species are as follows: *D. officinale* (Do), *A. thaliana* (At), *O. sativa* (Os), and *Z. mays* (Zm). Enzymes used for alignment were as follows: AtHDA6, AT5G63110; AtHDA19, AT4G38130; AtSRT1, AT5G55760; AtSRT2, AT5G09230; OsHDA704, Os07g0164100; OsHDA705, Os08g0344100; OsHDA706, Os06g0571100; OsHDA711, Os04g0409600; OsHDA712, Os05g0440100; OsHDA713, Os07g0602200; OsHDA714, Os12g0182700; OsHDT701, Os05g0597100; OsSRT701, Os04g0271000; OsSRT702, Os12g0179800, ZmHDA116, Zm00001d046388.

Full-size 🖼 DOI: 10.7717/peerj.10482/fig-5

elements, we selected some genes and used qRT-PCR to detect their expression patterns under various phytohormone treatments. We analyzed the expression patterns of 12 *DoHDAC* genes in different subfamilies after GA_3 treatment (Fig. 9). The results showed that after 4 h of GA_3 treatment, 11 genes in roots were highly up-regulated, *DoHDA8* and *DoHDA10* were the highest (> 20-fold), and *DoSRT2* was highly up-regulated in stems. In addition, after 24 h of GA_3 treatment, *DoHDA10* and *DoHDT4* were highly up-regulated in leaves. At the same time, *cis*-acting elements involved in the GA_3-response were found in
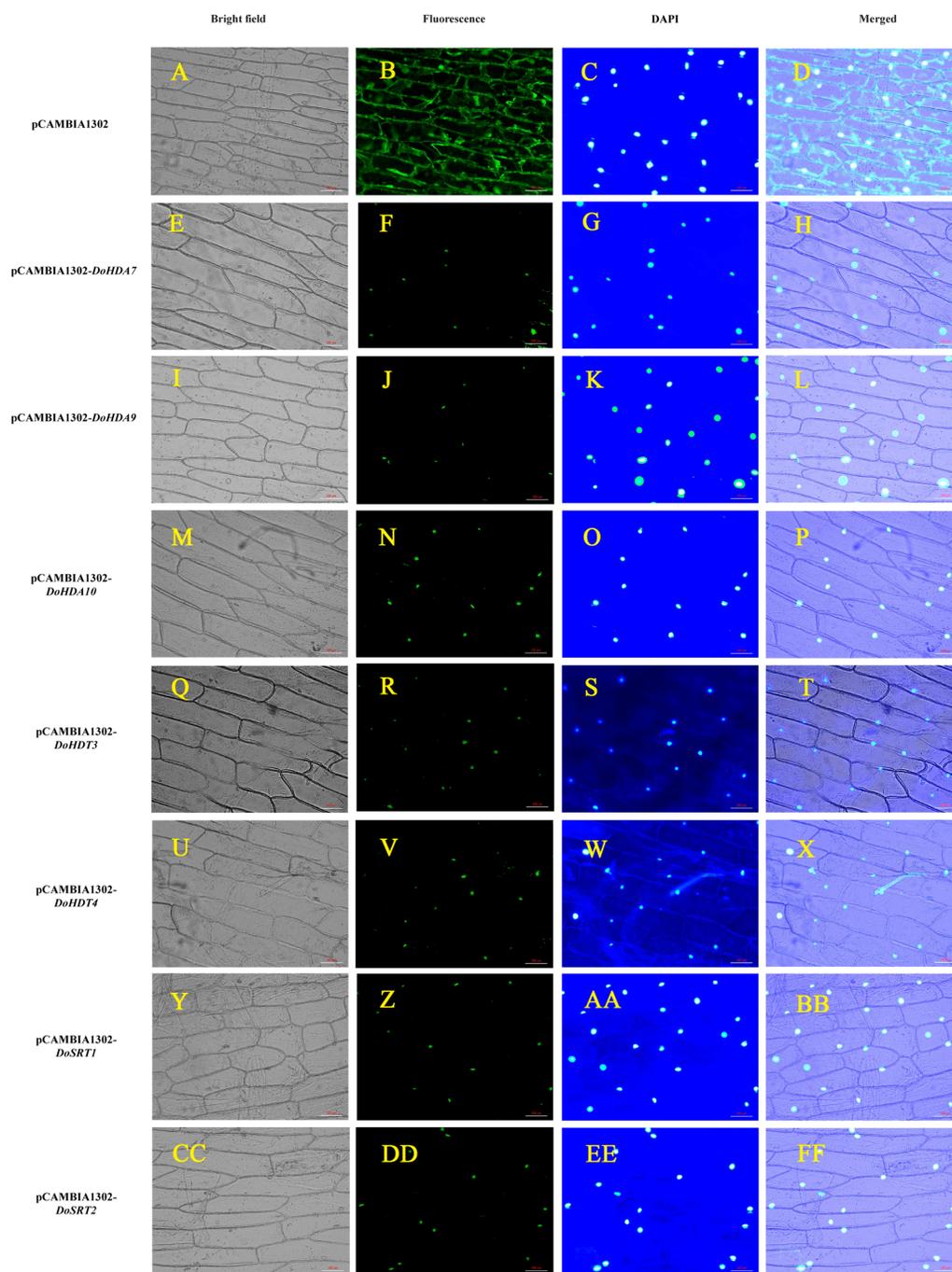
Figure 6 **Subcellular localization analysis of DoHDAC proteins.** pCAMBIA1302-*DoHDA7*, pCAMBIA1302-*DoHDA9*, pCAMBIA1302-*DoHDA10*, pCAMBIA1302-*DoHDT3*, pCAMBIA1302-*DoHDT4*, pCAMBIA1302-*DoSRT1* and pCAMBIA1302-*DoSRT2* was inserted into onion epidermal cells by *Agrobacterium*-mediated transformation to determine their subcellular localization. (A–D) GFP fluorescence distributed throughout the entire cells from the GFP empty vector. (continued on next page…)

Full-size 🖼 DOI: 10.7717/peerj.10482/fig-6

Zhang et al. (2020), *PeerJ*, DOI 10.7717/peerj.10482

12/30

Figure 6 (…continued)
(E–H) GFP fluorescence from cells expressing DoHDA7-GFP fusion protein localized to the nucleolus. (I–L) GFP fluorescence from cells expressing DoHDA9-GFP fusion protein localized to the nucleolus. (M–P) GFP fluorescence from cells expressing DoHDA10-GFP fusion protein localized to the nucleolus. (Q–T) GFP fluorescence from cells expressing DoHDT3-GFP fusion protein localized to the nucleolus. (U–X) GFP fluorescence from cells expressing DoHDT4-GFP fusion protein localized to the nucleolus. (Y–BB) GFP fluorescence from cells expressing DoSRT1-GFP fusion protein localized to the nucleolus. (CC–FF) GFP fluorescence from cells expressing DoSRT2-GFP fusion protein localized to the nucleolus. The panels from left to right correspond to brightfield, fluorescence (GFP), DAPI staining images and the merged images of fluorescence and brightfield, respectively. Scale bars: 100 µm.
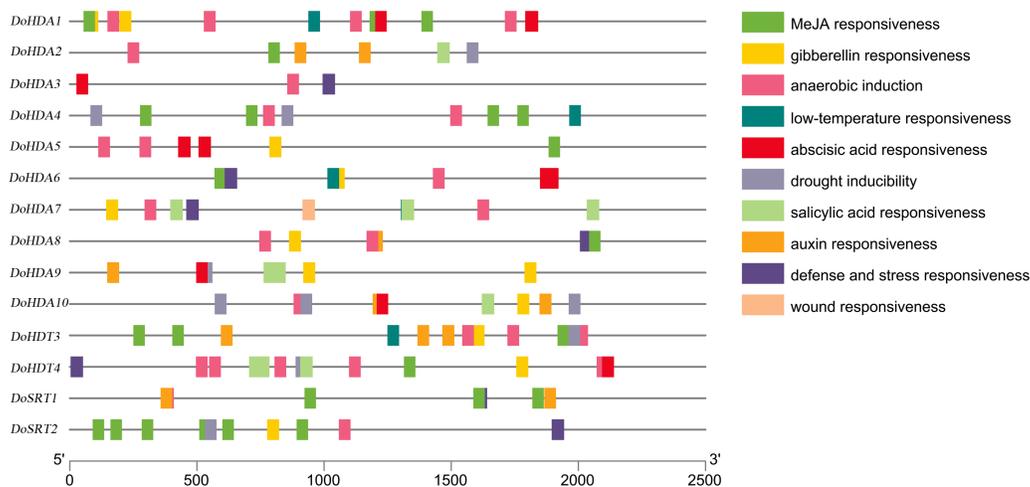
Figure 7 About 2 kb upstream sequences of *DoHDAC* genes and distribution of predicted *cis*-elements. Different *cis*-elements are represented using different colored boxes.

Full-size 🖼 DOI: 10.7717/peerj.10482/fig-7

these four genes (Table S2). Most selected *DoHDAC* genes were induced by exogenous SA treatment (Fig. 10). All genes in roots were highly up-regulated after 2 h under SA treatment, while the expression of *DoHDA10* and *DoHDT4* in leaves was highly up-regulated after 24 h of SA treatment. Moreover, *cis*-acting elements in response to SA were found in these two genes (Table S2). ABA is a widely distributed plant hormone in land plants and plays an important role in plant development (*Finkelstein, Gampala & Rock, 2002*). After 4 h of ABA treatment, 11 *DoHDAC* genes, especially *DoHDA8*, *DoHDA10* and *DoHDT4*, were up-regulated in roots (Fig. 11), and *cis*-acting elements in response to ABA were found in the promoters of *DoHDA8* and *DoHDT4* (Table S2). After 24 h of treatment with MeJA, 12 *DoHDAC* genes in roots were up-regulated and two *DoHDAC* genes were down-regulated (Fig. 12). Interestingly, we found that after 2 h of MeJA treatment, *DoHDA10* and *DoHDT4* were significantly up-regulated in stems and leaves (> 9-fold), and *cis*-acting elements in response to MeJA were found in the promoters of these two genes (Table S2). These results indicate that *DoHDT4* might be involved in GA$_3$-, SA-, ABA- and MeJA-mediated signal transduction pathways, *DoHDA10* might be involved in GA$_3$-, SA- and MeJA-mediated signal transduction pathways, and *DoHDA8* might be involved in ABA-mediated signal transduction pathways.
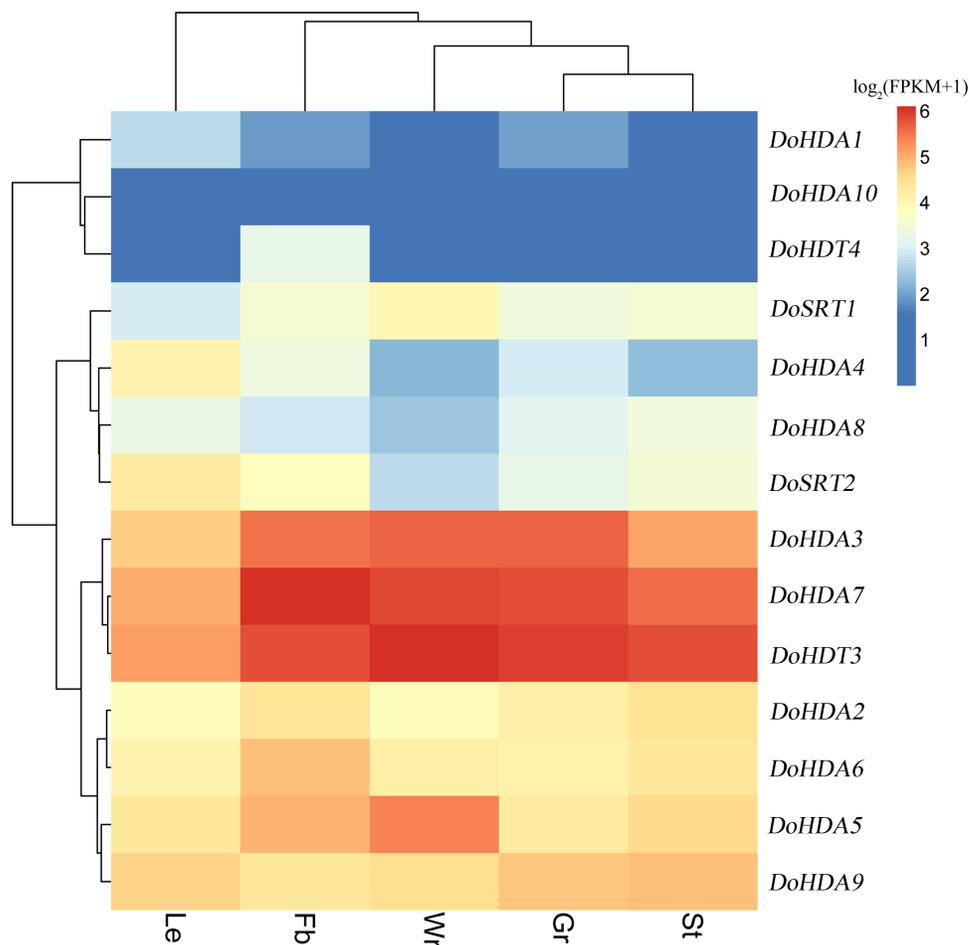
Figure 8 **Expression profiles of *DoHDAC* genes in different tissues based on the transcriptome data.** These data were used to analyze the expression profiles of *DoHDAC* genes in five different tissues: the white part of root (Wr), green root tip (Gr), stem (St), leaf (Le), and flower bud (Fb). The color bar represents the log_2(FKPM+1) values of each gene and transcript in different tissues. Red represents high relative expression, and blue represents low relative expression.

Full-size 🖼 DOI: 10.7717/peerj.10482/fig-8

Expression analysis of *DoHDAC* genes in response to abiotic stresses

HDAC proteins appear to activate positive and negative responses in salinity stress, with some discrepancies. For example, AtHDA9 and AtHD2D negatively regulate the salt response, whereas AtHDA6 and AtHD2C positively regulate it (*Ueda et al., 2017*). After salt (NaCl) treatment, most of the selected *DoHDAC* genes were highly up-regulated in leaves, especially *DoHDA10* and *DoHDT4*, which showed similar expression patterns (Fig. 13). After PEG treatment, most genes were highly up-regulated in roots, stems and leaves, especially *DoHDA10* and *DoHDT4*, which showed similar expression patterns (Fig. 14). In addition, *cis*-acting elements involved in responsiveness to drought were found in the promoters of *DoHDA10* and *DoHDT4* (Table S2). The drought stress response in plants is related to the status of histone acetylation. In response to drought stress, the level of acetylation of histone H3K9 increased in drought-responsive genes (*Kim*
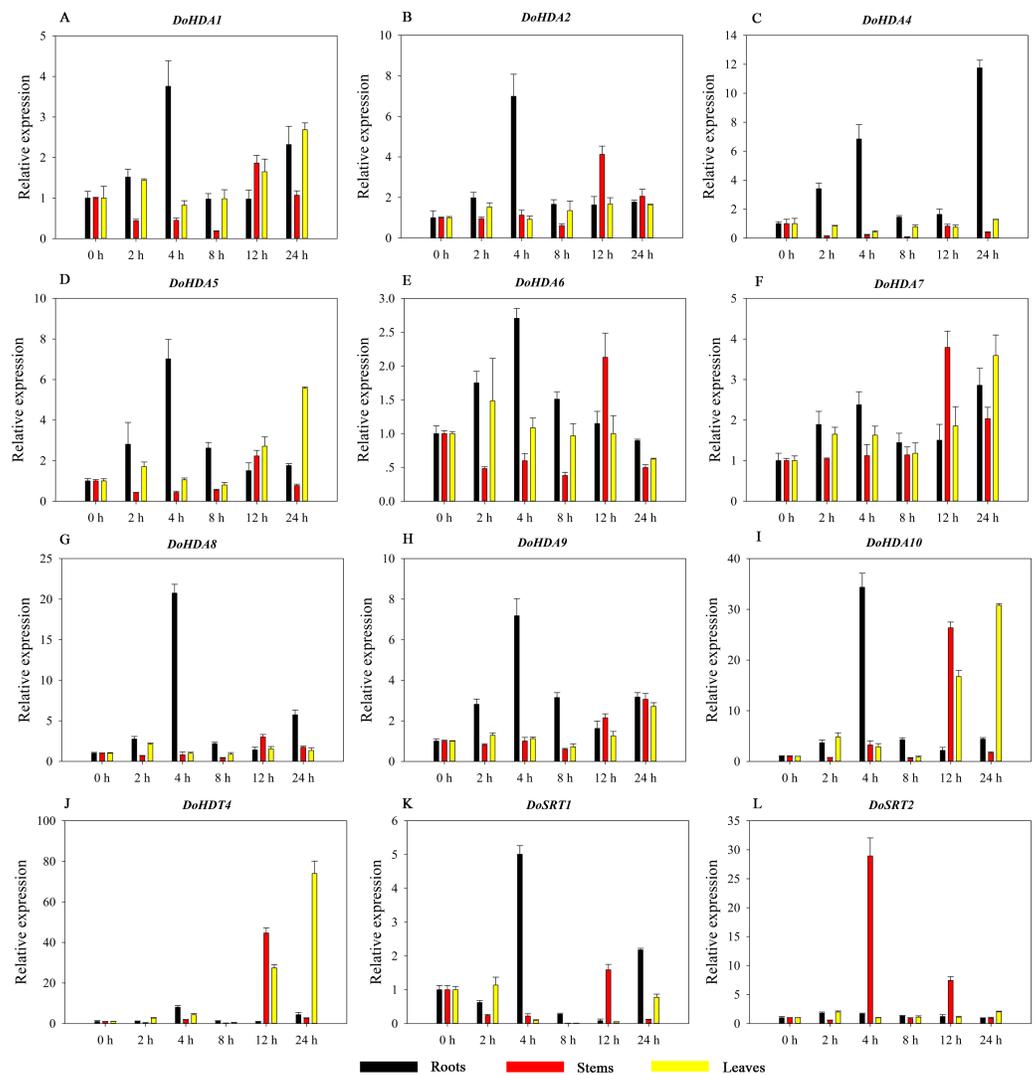
Figure 9 **Quantitative real-time reverse transcriptase-PCR analysis of expression of selected *DoHDAC* genes at different hours of GA₃ treatment in different tissues.** A–L represent *DoHDA1, DoHDA2, Do-HDA4, DoHDA5, DoHDA6, DoHDA7, DoHDA8, DoHDA9, DoHDA10, DoHDT4, DoSRT1, DoSRT2*, respectively. Error bars represent the standard error of the means of three independent replicates. Expression levels were calculated relative to 0 h of each organ.

Full-size ⬜ DOI: 10.7717/peerj.10482/fig-9

et al., 2008). Drought stress significantly induced four *HAT* genes in rice (*OsHAC703, OsHAG703, OsHAF701,* and *OsHAM701*) (*Fang et al., 2014*). However, in this study, the up-regulated expression of *DoHDAC* genes under drought stress may be related to the inhibited expression of drought-insensitive genes. *AtHD2C*-overexpressing *A. thaliana* plants showed ABA insensitivity, reduced transpiration, and enhanced tolerance to drought stress (*Sridha & Wu, 2006*). After low-temperature treatment, the selected *DoHDAC* genes were weakly up-regulated in roots, stems and leaves (Fig. 15). This is consistent with the expression of most *HDAC* genes in rice being regulated by salt and drought, but less affected by cold (*Hu et al., 2009*). Therefore, *DoHDA10* and *DoHDT4* might play an important role
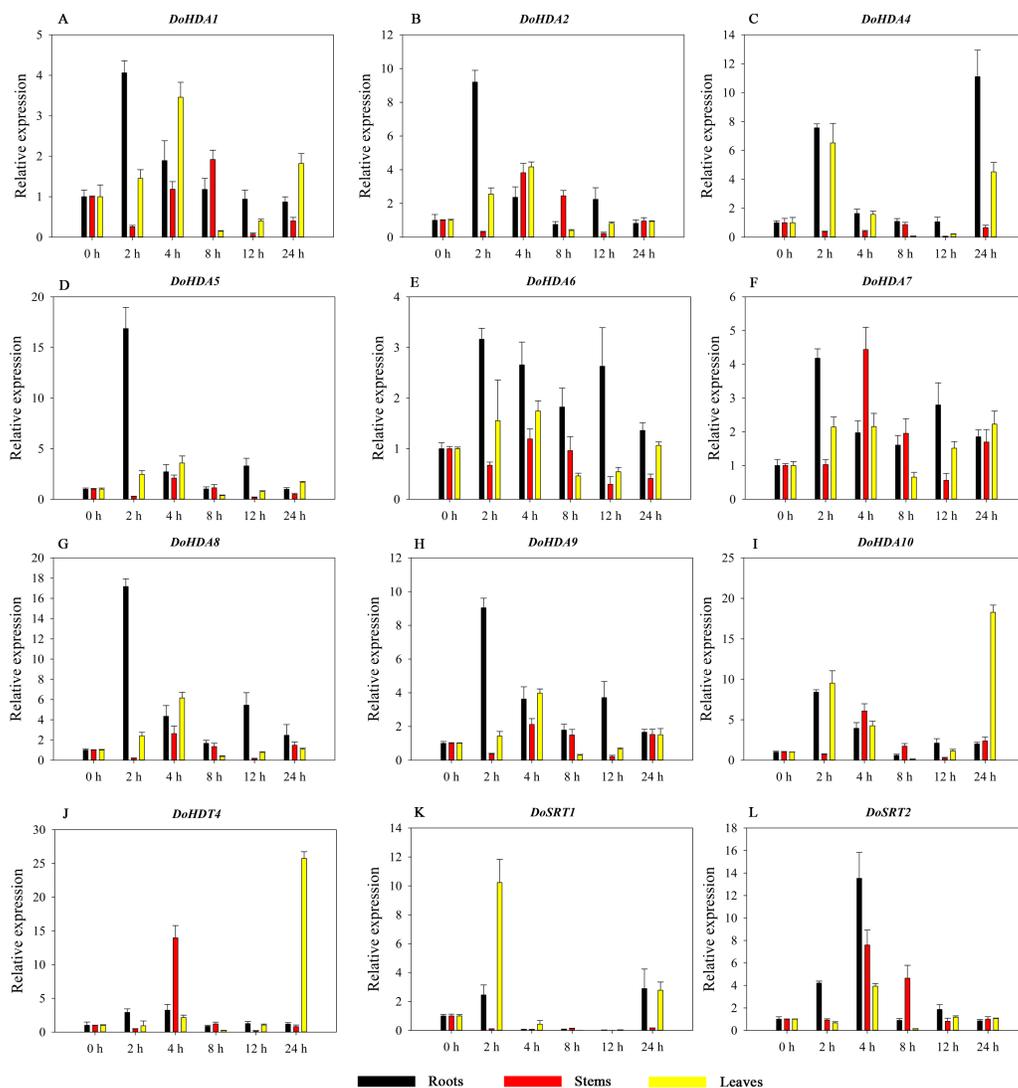
Figure 10 **Quantitative real-time reverse transcriptase-PCR analysis of expression of selected *Do-HDAC* genes at different hours of SA treatment in different tissues.** A–L represent *DoHDA1*, *DoHDA2*, *DoHDA4*, *DoHDA5*, *DoHDA6*, *DoHDA7*, *DoHDA8*, *DoHDA9*, *DoHDA10*, *DoHDT4*, *DoSRT1*, *DoSRT2*, respectively. Error bars represent the standard error of the means of three independent replicates. Expression levels were calculated relative to 0 h of each organ.

Full-size 🖼 DOI: 10.7717/peerj.10482/fig-10

in the regulation of salt and drought stress responses during the growth of *D. officinale* plants.

DISCUSSION

Plant HDAC proteins are a large family composed of multiple gene members. A variety of HDAC proteins have different subcellular localization and expression patterns, indicating that they have diverse functions. Reversible changes in histone deacetylation and acetylation play a crucial role in regulating gene expression involved in various developmental processes
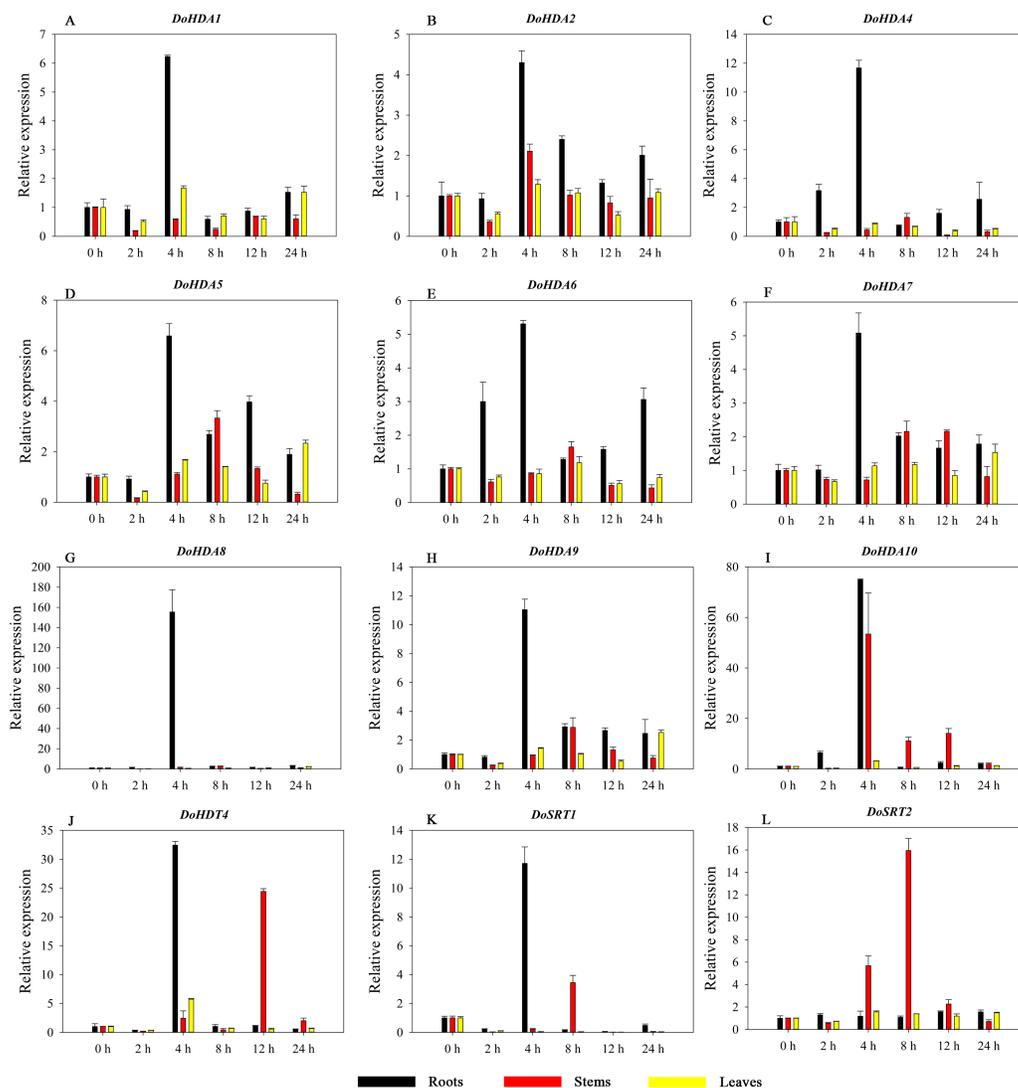
Figure 11 **Quantitative real-time reverse transcriptase-PCR analysis of expression of selected *DoHDAC* genes at different hours of ABA treatment in different tissues.** A–L represent *DoHDA1*, *DoHDA2*, *DoHDA4*, *DoHDA5*, *DoHDA6*, *DoHDA7*, *DoHDA8*, *DoHDA9*, *DoHDA10*, *DoHDT4*, *DoSRT1*, *DoSRT2*, respectively. Error bars represent the standard error of the means of three independent replicates. Expression levels were calculated relative to 0 h of each organ.

Full-size 🔲 DOI: 10.7717/peerj.10482/fig-11

and plant responses to abiotic stress (*Liu et al., 2014*). Plant HDAC proteins have been identified and characterized in some plant species such as *A. thaliana*, rice, soybean, tomato and others. For instance, a total of 18 AtHDAC proteins have been identified, 12 of which belong to the RPD3/HDA1 family, four belong to the HD2 family, and two belong to the SIR2 family (*Pandey et al., 2002*; *Wang et al., 2014*). Furthermore, at least 18 HDAC proteins have been identified in the rice genome, 14 of which belong to the RPD3/HDA1 family, two belong to the HD2 family, and two belong to the SIR2 family (*Hu et al., 2009*). In this study, we identified 14 HDAC proteins in *D. officinale* by using
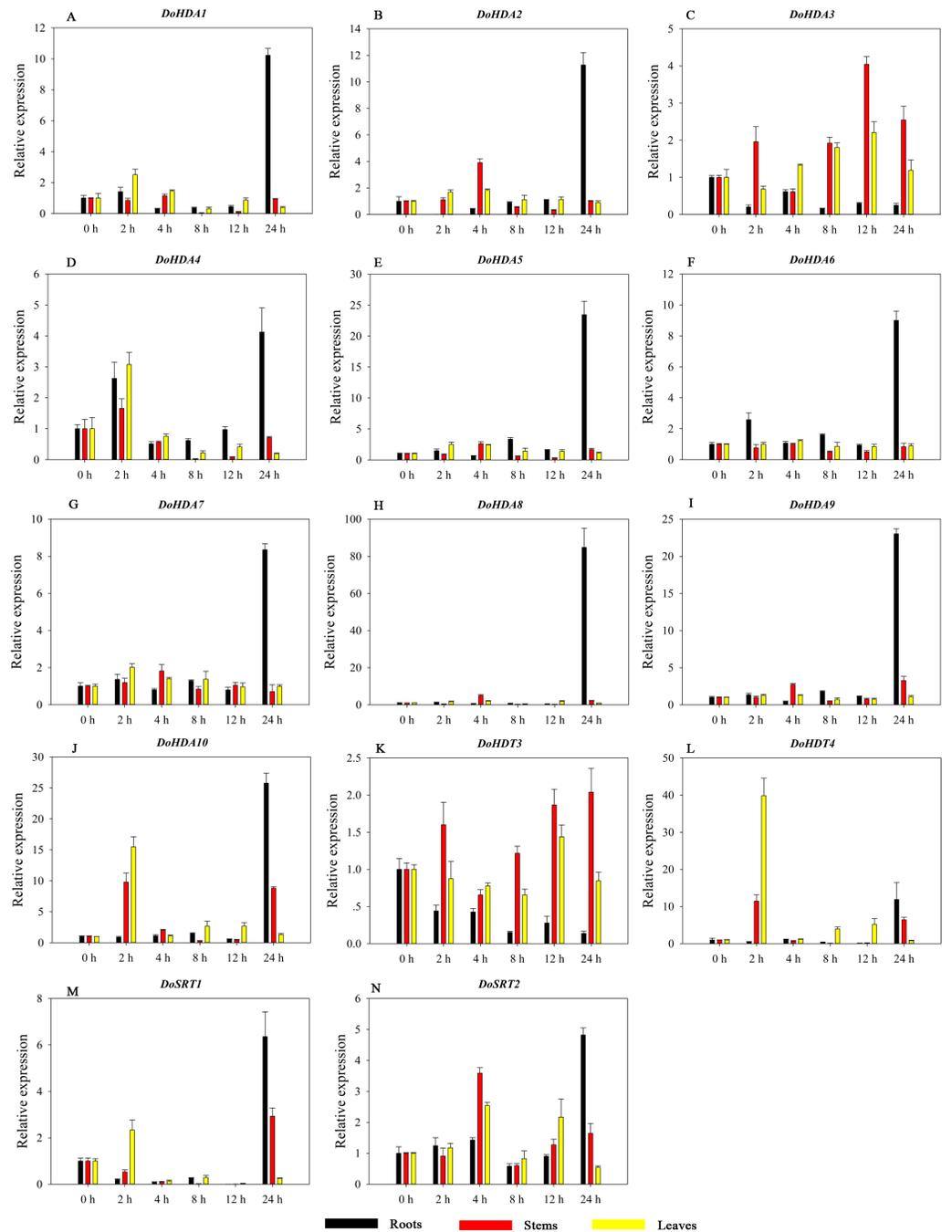
Figure 12 Quantitative real-time reverse transcriptase-PCR analysis of expression of selected *Do-HDAC* genes at different hours of MeJA treatment in different tissues. A–N represent *DoHDA1*, *Do-HDA2*, *DoHDA3*, *DoHDA4*, *DoHDA5*, *DoHDA6*, *DoHDA7*, *DoHDA8*, *DoHDA9*, *DoHDA10*, *DoHDT3*, *DoHDT4*, *DoSRT1*, *DoSRT2*, respectively. Error bars represent the standard error of the means of three independent replicates. Expression levels were calculated relative to 0 h of each organ.

Full-size 🖼 DOI: 10.7717/peerj.10482/fig-12
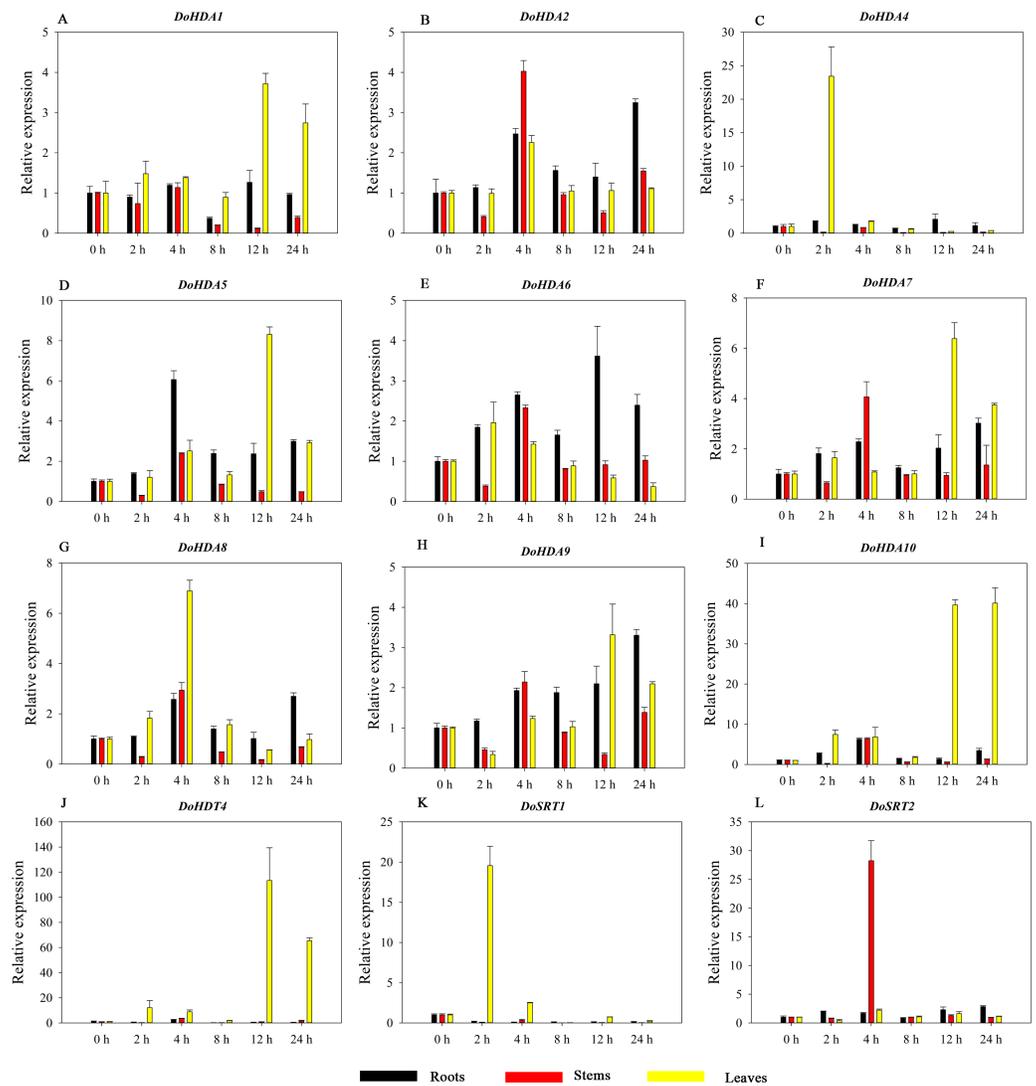
Figure 13 Quantitative real-time reverse transcriptase-PCR analysis of expression of selected _Do-HDAC_ genes at different hours of NaCl treatment in different tissues. A–L represent _DoHDA1_, _Do-HDA2_, _DoHDA4_, _DoHDA5_, _DoHDA6_, _DoHDA7_, _DoHDA8_, _DoHDA9_, _DoHDA10_, _DoHDT4_, _DoSRT1_, _DoSRT2_, respectively. Error bars represent the standard error of the means of three independent replicates. Expression levels were calculated relative to 0 h of each organ.

Full-size 🖼 DOI: 10.7717/peerj.10482/fig-13

bioinformatics analysis. However, the number of members of the HDAC proteins in _D. officinale_ identified was less than that in _A. thaliana_ and rice. The other DoHDAC proteins need to be identified and characterized in a future study.

Histone post-translational modifications (PTMs) are a major regulator of gene transcription. A number of PTMs are located within interfaces between H3/H4 tetramers and/or H2A/H2B dimers, such as the acetylation of H4(K91) (_Zhang et al., 2003_). Shortly after synthesis, histones H3 and H4 are acetylated by histone acetyltransferase 1/2 in the cytoplasm and then imported into the nucleus together with the histone acetyltransferase 1
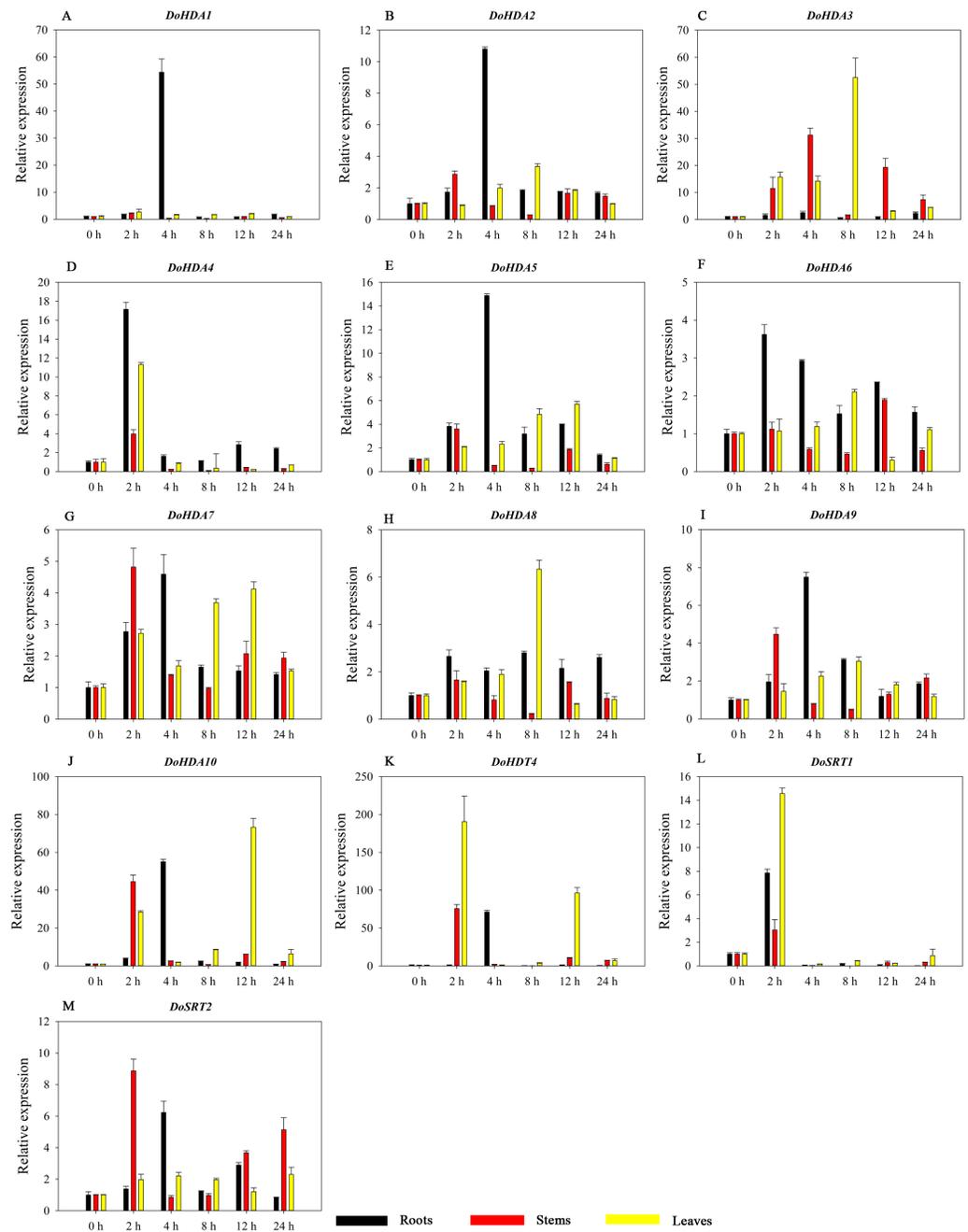
Figure 14 Quantitative real-time reverse transcriptase-PCR analysis of expression of selected *Do-HDAC* genes at different hours of PEG-6000 treatment in different tissues. A–M represent *DoHDA1*, *DoHDA2*, *DoHDA3*, *DoHDA4*, *DoHDA5*, *DoHDA6*, *DoHDA7*, *DoHDA8*, *DoHDA9*, *DoHDA10*, *DoHDT4*, *DoSRT1*, *DoSRT2*, respectively. Error bars represent the standard error of the means of three independent replicates. Expression levels were calculated relative to 0 h of each organ.

Full-size ⊡ DOI: 10.7717/peerj.10482/fig-14
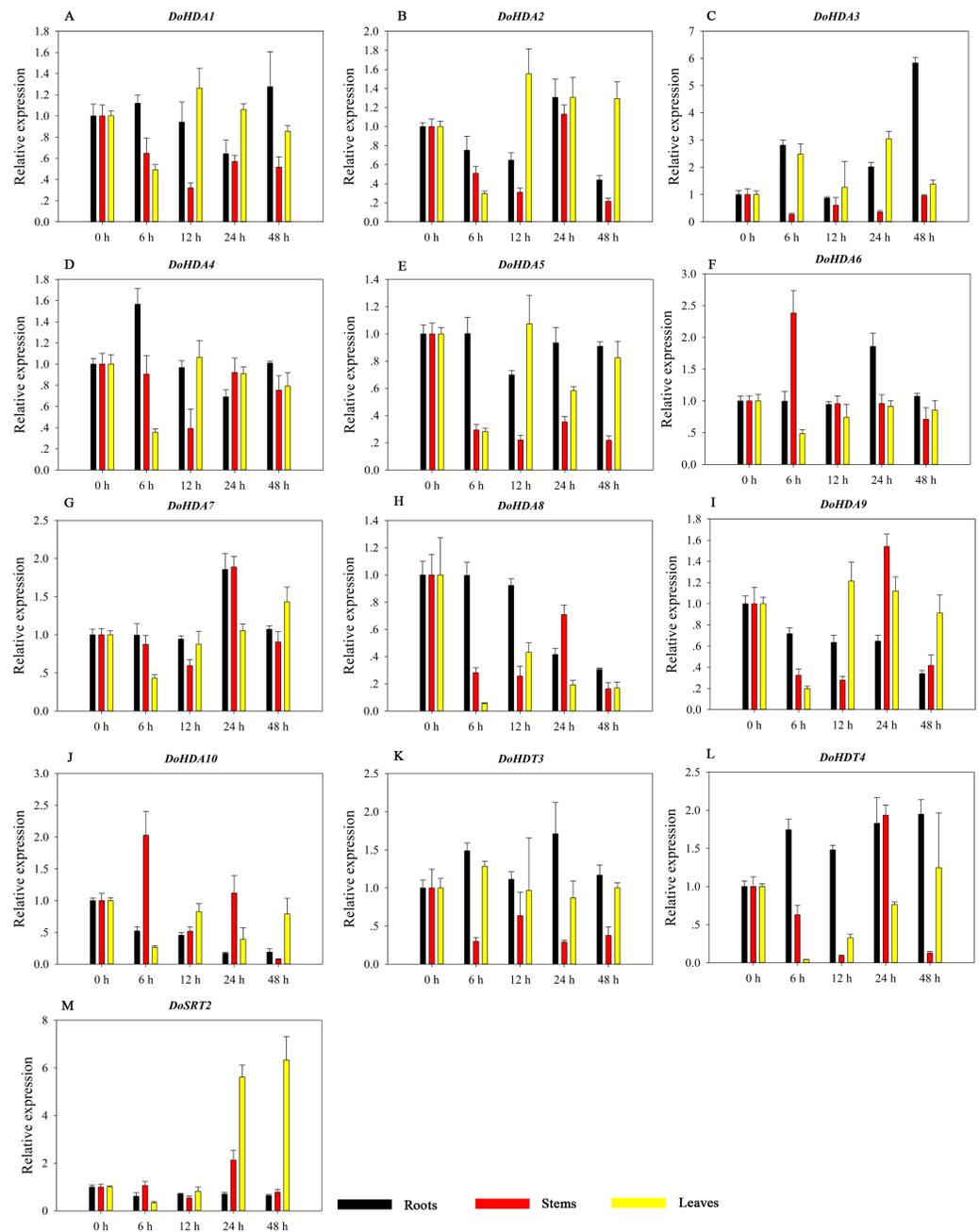
Figure 15 Quantitative real-time reverse transcriptase-PCR analysis of expression of selected *Do-HDAC* genes at different hours of cold (4 °C) treatment in different tissues. A–M represent *DoHDA1*, *DoHDA2*, *DoHDA3*, *DoHDA4*, *DoHDA5*, *DoHDA6*, *DoHDA7*, *DoHDA8*, *DoHDA9*, *DoHDA10*, *DoHDT3*, *DoHDT4*, *DoSRT2*, respectively. Error bars represent the standard error of the means of three independent replicates. Expression levels were calculated relative to 0 h of each organ.

Full-size 🖼 DOI: 10.7717/peerj.10482/fig-15

complex. In the nucleus, H3-H4 dimers or tetramers are recognized by chaperones such as CAF-1, Asf1 and Hif1, perhaps through their acetylation markers and are deposited together with histone H2A-H2B dimers onto newly replicated DNA to form nucleosomes, and then

rapidly deacetylated by histone deacetylase (*Shahbazian & Grunstein, 2007*). Moreover, some researches have shown that almost all acetyl-lysine-binding, bromodomain proteins (acetyl-lysine readers) are localized in the nucleus, and many of them are directly involved in the regulation of transcription (*Narita, Weinert & Choudhary, 2019*). Therefore, most HDAC proteins were localized in the nucleus in this study, which may be related to their function of removing acetyl groups from histones. The localization of HDAC proteins are also diverse in different environments. Some HDAC proteins are shuttled between the cytoplasm and the nucleus. For example, AtHDA15 shuttled from the cytoplasm to the nucleus in the presence of light, but exported out of the nucleus in darkness, implying that it could participate in the light signaling pathway (*Alinsug et al., 2012*). Moreover, the localization of HDAC proteins is variable in different plant tissues. For an instance, in anthers/endosperm, maize ZmHDA108 was localized in the nucleus and cytoplasm, while in shoot apexes, it was mainly found in the cytoplasm (*Varotto et al., 2003*). The green fluorescence of the DoHDA7-GFP and DoHDA9-GFP fusions were observed in the nucleus by *Agrobacterium*-mediated transient transformation used in onion epidermal cells (Fig. 6). Similarly, AtHDA6 and AtHDA19 was localized in the nucleus, which was consistent with the roles of these proteins as HDAC proteins (*Kurita et al., 2019*; *Wu et al., 2008*; *Zhou et al., 2005*). It should be noted, however, that the subcellular localization assays in the present study were performed using onion epidermal cells, and therefore, it is entirely possible that *D. officinale*-specific interactions could affect the localization pattern *in situ*.

Zinc finger proteins are a class of important transcription factors that regulate plant cell development (*Sun et al., 2015*). According to the number and position of cysteine residues and histidine residues, which bind zinc ions in the secondary structure of fingers, zinc finger proteins are classified into several types: C_2H_2, C_2C_2, C_2HC, $C_2C_2C_2C_2$, and $C_2HCC_2C_2$ (*Ciftci-Yilmaz & Mittler, 2008*). Among them, the C_2H_2-type zinc finger proteins are one of the most important groups and are involved in downstream gene regulation (*Sakamoto et al., 2000*; *Tague, Gallant & Goodman, 1996*). They are mainly involved in regulating biological processes such as plant branch and flower development, stress response and hormone signaling pathways (*Sun et al., 2015*). In this study, a typical C_2H_2-type zinc finger domain was found on the C-terminus of DoHDT3 (Fig. 2). Therefore, DoHDT3 might interact with other proteins to regulate plant development and stress response. AtHDA6 and AtHDA19 are the most well-studied RPD3/HDA1 family of HDAC proteins in plants, and they play a vital role in the growth and development of plants (*Alinsug, Yu & Wu, 2009*). Flowering is vital for plants to complete the life cycle and produce offspring. AtHDA6 and AtHDA19 are global repressors involved in flowering or flower development (*Alinsug, Yu & Wu, 2009*). Due to the high sequence similarity between DoHDA9 and AtHDA6 and between DoHDA7 and AtHDA19, DoHDA7 and DoHDA9 may have similar functions in regulating plant development as their homologs in *A. thaliana*. For example, when *AtHDA6* is suppressed, the expression of jasmonate-responsive genes is down-regulated (*Wu et al., 2008*). Similarly, after MeJA treatment, the expression level of *DoHDA9* was up-regulated in roots (Fig. 12). *AtHDA19* plays a pivotal role in tolerance to salinity stress (*Ueda et al., 2017*). Correspondingly, after NaCl treatment, the expression

level of *DoHDA7* was up-regulated in stems and leaves (Fig. 13). The expression of *HDAC* genes occurs in response to stresses and is regulated by stress-related hormones like SA, JA or ABA (*Fu, Wu & Duan, 2007*; *Hu et al., 2009*). ABA is the plant hormone most directly involved in stress signal transduction (*Xiong, Schumaker & Zhu, 2002*). JA generally inhibits plant growth and promotes defense responses against insect pests and pathogens while ABA is involved in the water stress response, regulating plant water balance and osmotic stress tolerance (*Ma et al., 2013*). After ABA treatment, the expression levels of *AtHD2C*, which is a synonym of *AtHDT3*, *OsHDT701*, *OsHTD702*, *OsSRT701* and *OsSRT702* were down-regulated (*Fu, Wu & Duan, 2007*; *Sridha & Wu, 2006*). In contrast, the expression levels of *DoHDA10*, *DoHDT4*, and *DoSRT1* were significantly up-regulated in roots after ABA treatment and in leaves after NaCl treatment (Figs. 11 & 13), so they may affect the expression level of some stress-responsive genes. In addition to their functions in plant development and stress responses, HDAC proteins are also involved in cellular processes such as cell death. OsSRT1 in rice and NtHD2a and NtHD2b in tobacco act as negative regulators of cell death (*Bourque et al., 2011*; *Huang et al., 2007*). Programmed cell death (PCD) in the maize aleurone layer is induced by GA, and HDAC activity is required for this process. HDAC activity gradually increased relative to histone acetyltransferase (HAT) activity, leading to a global decrease in histone H3 and H4 acetylation levels during PCD after treatment with GA (*Hou et al., 2017*). These data further prove that the *DoHDAC* genes play an important role in the growth and development of *D. officinale* and in response to environmental stresses. Further research is required to identify proteins that interact with DoHDAC proteins and their global targets in *D. officinale*.

CONCLUSIONS

We comprehensively identified and analyzed the *HDAC* genes from *D. officinale*. We performed a phylogenetic analysis, as well as analyses of conserved motifs, *cis*-acting elements, gene structure, protein interactions, and subcellular localization of some *DoHDAC* genes. These results help to elucidate the classification and function of the *DoHDAC* genes. Expression pattern analysis in different tissues showed that the *DoHDAC* genes were widely expressed in roots, stems, leaves and flower buds. The expression pattern of *DoHDAC* genes under abiotic stresses and various phytohormone treatments show that some *DoHDAC* genes were modulated by abiotic stresses such as salt, cold and drought, as well as plant hormones such as GA_3, SA, ABA and MeJA. In summary, this information about the *HDAC* genes in *D. officinale* helps to reveal their role in epigenetic regulation of plant growth, development, and response to stresses.

ADDITIONAL INFORMATION AND DECLARATIONS

Competing Interests

The authors declare that they have no competing interests.

Author Contributions

- Mingze Zhang performed the experiments, prepared figures and/or tables, authored or reviewed drafts of the paper, and approved the final draft.
- Jaime A. Teixeira da Silva analyzed the data, authored or reviewed drafts of the paper, and approved the final draft.
- Zhenming Yu, Haobin Wang, Can Si and Conghui Zhao analyzed the data, prepared figures and/or tables, and approved the final draft.
- Chunmei He and Jun Duan conceived and designed the experiments, authored or reviewed drafts of the paper, and approved the final draft.

Data Deposition

The following information was supplied regarding data availability:
The raw data are available in the Supplemental File.

Supplemental Information

Supplemental information for this article can be found online at http://dx.doi.org/10.7717/peerj.10482#supplemental-information.

REFERENCES

Alinsug MV, Chen F, Luo M, Tai R, Jiang L, Wu K. 2012. Subcellular localization of Class II HDAs in *Arabidopsis thaliana*: nucleocytoplasmic shuttling of HDA15 is driven by light. *PLOS ONE* **7**:e30846 DOI 10.1371/journal.pone.0030846.

Alinsug MV, Yu C, Wu K. 2009. Phylogenetic analysis, subcellular localization, and expression patterns of RPD3/HDA1 family histone deacetylases in plants. *BMC Plant Biology* **9**:37 DOI 10.1186/1471-2229-9-37.

Ashraf MA, Iqbal M, Rasheed R, Hussain I, Riaz M, Arif MS. 2018. Chapter 8—environmental stress and secondary metabolites in plants: an overview. In: Ahmad P, Ahanger MA, Singh VP, Tripathi DK, Alam P, Alyemeni MN, eds. *Plant metabolites and regulation under environmental stress.* London: Academic Press, 153–167 DOI 10.1016/B978-0-12-812689-9.00008.

Bailey TL, Boden M, Buske FA, Frith M, Grant CE, Clementi L, Ren J, Li WW, Noble WS. 2009. MEME SUITE: tools for motif discovery and searching. *Nucleic Acids Research* **37**:W202–W208 DOI 10.1093/nar/gkp335.

Ballare CL, Austin AT. 2019. Recalculating growth and defense strategies under competition: key roles of photoreceptors and jasmonates. *Journal of Experimental Botany* **70**:3425–3434 DOI 10.1093/jxb/erz237.

Berger SL. 2007. The complex language of chromatin regulation during transcription. *Nature* **447**:407–412 DOI 10.1038/nature05915.

Bourque S, Dutartre A, Hammoudi V, Blanc S, Dahan J, Jeandroz S, Pichereaux C, Rossignol M, Wendehenne D. 2011. Type-2 histone deacetylases as new regulators of elicitor-induced cell death in plants. *New Phytologist* **192**:127–139 DOI 10.1111/j.1469-8137.2011.03788.x.

Busconi M, Reggi S, Fogher C, Bavaresco L. 2009. Evidence of a sirtuin gene family in grapevine (*Vitis vinifera* L.). *Plant Physiology and Biochemistry* **47**:650–652 DOI 10.1016/j.plaphy.2009.03.003.

Chen C, Chen H, Zhang Y, Thomas HR, Frank MH, He Y, Xia R. 2020. TBtools: an integrative toolkit developed for interactive analyses of big biological data. *Molecular Plant* **13**:1194–1202 DOI 10.1016/j.molp.2020.06.009.

Chen L, Wu K. 2010. Role of histone deacetylases HDA6 and HDA19 in ABA and abiotic stress response. *Plant Signaling and Behavior* **5**:1318–1320 DOI 10.4161/psb.5.10.13168.

Chen X, Wang F, Wang Y, Li X, Wang A, Wang C, Guo S. 2012. Discrimination of the rare medicinal plant *Dendrobium officinale* based on naringenin, bibenzyl, and polysaccharides. *Science China—Life Sciences* **55**:1092–1099 DOI 10.1007/s11427-012-4419-3.

Chu J, Chen Z. 2018. Molecular identification of histone acetyltransferases and deacetylases in lower plant *Marchantia polymorpha*. *Plant Physiology and Biochemistry* **132**:612–622 DOI 10.1016/j.plaphy.2018.10.012.

Ciftci-Yilmaz S, Mittler R. 2008. The zinc finger network of plants. *Cellular and Molecular Life Sciences* **65**:1150–1160 DOI 10.1007/s00018-007-7473-4.

Demetriou K, Kapazoglou A, Tondelli A, Francia E, Stanca MA, Bladenopoulos K, Tsaftaris AS. 2009. Epigenetic chromatin modifiers in barley: I. Cloning, mapping and expression analysis of the plant specific HD2 family of histone deacetylases from barley, during seed development and after hormonal treatment. *Physiologia Plantarum* **136**:358–368 DOI 10.1111/j.1399-3054.2009.01236.x.

Ding J, Tu H, Zang Z, Huang M, Zhou S. 2018. Precise control and prediction of the greenhouse growth environment of *Dendrobium candidum*. *Computers Electronics in Agriculture* **151**:453–459 DOI 10.1016/j.compag.2018.06.037.

Fang H, Liu X, Thorn G, Duan J, Tian L. 2014. Expression analysis of histone acetyltransferases in rice under drought stress. *Biochemical and Biophysical Research Communications* **443**:400–405 DOI 10.1016/j.bbrc.2013.11.102.

Feng K, Liu F, Zou J, Xing G, Deng P, Song W, Tong W, Nie X. 2016. Genome-wide identification, evolution, and co-expression network analysis of mitogen-activated protein kinase kinase kinases in *Brachypodium distachyon*. *Frontiers in Plant Science* **7**:1400 DOI 10.3389/fpls.2016.01400.

Finkelstein RR, Gampala SS, Rock CD. 2002. Abscisic acid signaling in seeds and seedlings. *The Plant Cell* **14**:S15–S45 DOI 10.1105/tpc.010441.

Forestan C, Farinati S, Rouster J, Lassagne H, Lauria M, Dal Ferro N, Varotto S. 2018. Control of maize vegetative and reproductive development, fertility, and rRNAs silencing by histone deacetylase 108. *Genetics* **208**:1443–1466 DOI 10.1534/genetics.117.300625.

Fu CC, Han YC, Guo YF, Kuang JF, Chen JY, Shan W, Lu WJ. 2018. Differential expression of histone deacetylases during banana ripening and identification of MaHDA6 in regulating ripening-associated genes. *Postharvest Biology and Technology* **141**:24–32 DOI 10.1016/j.postharvbio.2018.03.010.

Fu W, Wu K, Duan J. 2007. Sequence and expression analysis of histone deacetylases in rice. *Biochemical and Biophysical Research Communications* **356**:843–850 DOI 10.1016/j.bbrc.2007.03.010.

Grunstein M. 1997. Histone acetylation in chromatin structure and transcription. *Nature* **389**:349–352 DOI 10.1038/38664.

Hayford RKA, Ligaba-Osena A, Subramani M, Brown A, Melmaiee K, Hossain K, Kalavacharla VK. 2017. Characterization and expression analysis of common bean histone deacetylase 6 during development and cold stress response. *International Journal of Genomics* **2017**:349–352 DOI 10.1155/2017/2502691.

He C, Zeng S, Teixeira da Silva JA, Yu Z, Tan J, Duan J. 2017. Molecular cloning and functional analysis of the *phosphomannomutase* (*PMM*) gene from *Dendrobium officinale* and evidence for the involvement of an abiotic stress response during germination. *Protoplasma* **254**:1693–1704 DOI 10.1007/s00709-016-1044-1.

He C, Zhang J, Liu X, Zeng S, Wu K, Yu Z, Wang X, Teixeira da Silva JA, Lin Z, Duan J. 2015. Identification of genes involved in biosynthesis of mannan polysaccharides in *Dendrobium officinale* by RNA-seq analysis. *Plant Molecular Biology* **88**:219–231 DOI 10.1007/s11103-015-0316-z.

Hirschey MD. 2011. Old enzymes, new tricks: sirtuins are NAD^{+}-dependent de-*acylases*. *Cell Metabolism* **14**:718–719 DOI 10.1016/j.cmet.2011.10.006.

Hollender C, Liu Z. 2008. Histone deacetylase genes in *Arabidopsis* development. *Journal of Integrative Plant Biology* **50**:875–885 DOI 10.1111/j.1744-7909.2008.00704.x.

Hou H, Zheng X, Zhang H, Yue M, Li L. 2017. Histone deacetylase is required for GA-induced programmed cell death in maize aleurone layers. *Plant Physiology* **175**:1484–1496 DOI 10.1104/pp.17.00953.

Hu B, Jin J, Guo AY, Zhang H, Luo J, Gao G. 2014. GSDS 2.0: an upgraded gene feature visualization server. *Bioinformatics* **31**:1296–1297 DOI 10.1093/bioinformatics/btu817.

Hu Y, Qin F, Huang L, Sun Q, Li C, Zhao Y, Zhou DX. 2009. Rice histone deacetylase genes display specific expression patterns and developmental functions. *Biochemical and Biophysical Research Communications* **388**:266–271 DOI 10.1016/j.bbrc.2009.07.162.

Huang L, Sun Q, Qin F, Li C, Zhao Y, Zhou D. 2007. Down-regulation of a SILENT INFORMATION REGULATOR2-related histone deacetylase gene, *OsSRT1*,

induces DNA fragmentation and cell death in rice. *Plant Physiology* **144**:1508–1519 DOI 10.1104/pp.107.099473.

Huang XS, Luo T, Fu XZ, Fan QJ, Liu JH. 2011. Cloning and molecular characterization of a mitogen-activated protein kinase gene from *Poncirus trifoliata* whose ectopic expression confers dehydration/drought tolerance in transgenic tobacco. *Journal of Experimental Botany* **62**:5191–5206 DOI 10.1093/jxb/err229.

Juswara LS, Schuiteman A, Champion J. 2019. *Dendrobium annulatum* (Orchidaceae: Epidendroideae), a new species of *Dendrobium* section *Grastidium* from Indonesian New Guinea. *Phytotaxa* **414**:151–155 DOI 10.11646/phytotaxa.414.3.4.

Khan MIR, Fatma M, Per TS, Anjum NA, Khan NA. 2015. Salicylic acid-induced abiotic stress tolerance and underlying mechanisms in plants. *Frontiers in Plant Science* **6**:462 DOI 10.3389/fpls.2015.00462.

Kim JM, Sasaki T, Ueda M, Sako K, Seki M. 2010. Chromatin regulation functions in plant abiotic stress responses. *Plant Cell and Environment* **33**:604–611 DOI 10.1111/j.1365-3040.2009.02076.x.

Kim JM, Sasaki T, Ueda M, Sako K, Seki M. 2015. Chromatin changes in response to drought, salinity, heat, and cold stresses in plants. *Frontiers in Plant Science* **6**:114 DOI 10.3389/fpls.2015.00114.

Kim J, To TK, Ishida J, Morosawa T, Kawashima M, Matsui A, Toyoda T, Kimura H, Shinozaki K, Seki M. 2008. Alterations of lysine modifications on the histone H3 N-tail under drought stress conditions in *Arabidopsis thaliana*. *Plant Cell Physiology* **49**:1580–1588 DOI 10.1093/pcp/pcn133.

Kumar S, Stecher G, Tamura K. 2016. MEGA7: molecular evolutionary genetics analysis version 7.0 for bigger datasets. *Molecular Biology and Evolution* **33**:1870–1874 DOI 10.1093/molbev/msw054.

Kurita K, Sakamoto Y, Naruse S, Matsunaga TM, Arata H, Higashiyama T, Habu Y, Utsumi Y, Utsumi C, Tanaka M, Takahashi S, Kim JM, Seki M, Sakamoto T, Matsunaga S. 2019. Intracellular localization of histone deacetylase HDA6 in plants. *Journal of Plant Research* **132**:629–640 DOI 10.1007/s10265-019-01124-8.

Lagacé M, Chantha SC, Major G, Matton DP. 2003. Fertilization induces strong accumulation of a histone deacetylase (HD2) and of other chromatin-remodeling proteins in restricted areas of the ovules. *Plant Molecular Biology* **53**:759–769 DOI 10.1023/B:PLAN.0000023665.36676.8.

Larkin MA, Blackshields G, Brown N, Chenna R, McGettigan PA, McWilliam H, Valentin F, Wallace IM, Wilm A, Lopez R. 2007. Clustal W and Clustal X version 2.0. *Bioinformatics* **23**:2947–2948 DOI 10.1093/bioinformatics/btm404.

Li J, Li S, Huang D, Zhao X, Cai G. 2011. Advances in the of resources, constituents and pharmacological effects of *Dendrobium officinale*. *Keji Daobao / Science and Technology Review* **29**:74–79 DOI 10.3981/j.issn.1000-7857.2011.18.012.

Li Z, Peng R, Tian Y, Han H, Xu J, Yao Q. 2016. Genome-wide identification and analysis of the myb transcription factor superfamily in *Solanum lycopersicum*. *Plant Cell Physiology* **57**:1657–1677 DOI 10.1093/pcp/pcw091.

Liu X, Yang S, Zhao M, Luo M, Yu CW, Chen CY, Tai R, Wu K. 2014. Transcriptional repression by histone deacetylases in plants. *Molecular Plant* **7**:764–772 DOI 10.1093/mp/ssu033.

Livak KJ, Schmittgen TD. 2001. Analysis of relative gene expression data using real-time quantitative PCR and the $2^{-\Delta\Delta CT}$ method. *Methods* **25**:402–408 DOI 10.1006/meth.2001.1262.

Luger K, Mäder AW, Richmond RK, Sargent DF, Richmond TJ. 1997. Crystal structure of the nucleosome core particle at 2.8 Å resolution. *Nature* **389**:251–260 DOI 10.1038/38444.

Ma X, Lv S, Zhang C, Yang C. 2013. Histone deacetylases and their functions in plants. *Plant Cell Reports* **32**:465–478 DOI 10.1007/s00299-013-1393-6.

Murashige T, Skoog F. 1962. A revised medium for rapid growth and bioassay with tobacco tissue cultures. *Physiologia Plantarum* **15**:473–497 DOI 10.1111/j.1399-3054.1962.tb08052.x.

Narita T, Weinert BT, Choudhary C. 2019. Functions and mechanisms of non-histone protein acetylation. *Nature Reviews Molecular Cell Biology* **20**:156–174 DOI 10.1038/s41580-018-0081-3.

Pandey R, Müller A, Napoli CA, Selinger DA, Pikaard CS, Richards EJ, Bender J, Mount DW, Jorgensen RA. 2002. Analysis of histone acetyltransferase and histone deacetylase families of *Arabidopsis thaliana* suggests functional diversification of chromatin modification among multicellular eukaryotes. *Nucleic Acids Research* **30**:5036–5055 DOI 10.1093/nar/gkf660.

Peng M, Ying P, Liu X, Li C, Xia R, Li J, Zhao M. 2017. Genome-wide identification of histone modifiers and their expression patterns during fruit abscission in litchi. *Frontiers in Plant Science* **8**:639 DOI 10.3389/fpls.2017.00639.

Ramakrishna A, Ravishankar GA. 2011. Influence of abiotic stress signals on secondary metabolites in plants. *Plant Signaling & Behavior* **6**:1720–1731 DOI 10.4161/psb.6.11.17613.

Ren J, Wen L, Gao X, Jin C, Xue Y, Yao X. 2009. DOG 1.0: illustrator of protein domain structures. *Cell Research* **19**:271–273 DOI 10.1038/cr.2009.6.

Sakamoto H, Araki T, Meshi T, Iwabuchi M. 2000. Expression of a subset of the *Arabidopsis* Cys_2/His_2-type zinc-finger protein gene family under water stress. *Gene* **248**:23–32 DOI 10.1016/S0378-1119(00)00133-5.

Shahbazian MD, Grunstein M. 2007. Functions of site-specific histone acetylation and deacetylation. *Annual Review of Biochemistry* **76**:75–100 DOI 10.1146/annurev.biochem.76.052705.162114.

Shao H, Wang H, Tang X. 2015. NAC transcription factors in plant multiple abiotic stress responses: progress and prospects. *Frontiers in Plant Science* **6**:902 DOI 10.3389/fpls.2015.00902.

Shen C, Guo H, Chen H, Shi Y, Meng Y, Lu J, Feng S, Wang H. 2017. Identification and analysis of genes associated with the synthesis of bioactive constituents in *Dendrobium officinale* using RNA-Seq. *Scientific Reports* **7**:187 DOI 10.1038/s41598-017-00292-8.

Teixeira da Silva JA, Ng TB. 2017. The medicinal and pharmaceutical importance of *Dendrobium* species. *Applied Microbiology and Biotechnology* **101**:2227–2239 DOI 10.1007/s00253-017-8169-9.

Sperschneider J, Catanzariti AM, DeBoer K, Petre B, Gardiner DM, Singh KB, Dodds PN, Taylor JM. 2017. LOCALIZER: subcellular localization prediction of both plant and effector proteins in the plant cell. *Scientific Reports* **7**:44598 DOI 10.1038/srep44598.

Sridha S, Wu K. 2006. Identification of *AtHD2C* as a novel regulator of abscisic acid responses in *Arabidopsis*. *The Plant Journal* **46**:124–133 DOI 10.1111/j.1365-313X.2006.02678.x.

Srivastava R, Singh UM, Dubey NK. 2016. Histone modifications by different histone modifiers: insights into histone writers and erasers during chromatin modification. *Journal of Biological Sciences and Medicine* **2**:45–54 DOI 10.5005/jp-journals-10045-0035.

Sun L, Zhang A, Zhou Z, Zhao Y, Yan A, Bao S, Yu H, Gan Y. 2015. *GLABROUS INFLORESCENCE STEMS 3* (*GIS 3*) regulates trichome initiation and development in *Arabidopsis*. *New Phytologist* **206**:220–230 DOI 10.1111/nph.13218.

Szklarczyk D, Gable AL, Lyon D, Junge A, Wyder S, Huerta-Cepas J, Simonovic M, Doncheva NT, Morris JH, Bork P, Jensen LJ, Mering CV. 2019. STRING v11: protein-protein association networks with increased coverage, supporting functional discovery in genome-wide experimental datasets. *Nucleic Acids Research* **47**:D607–D613 DOI 10.1093/nar/gky1131.

Tague BW, Gallant P, Goodman HM. 1996. Expression analysis of an *Arabidopsis* C_2H_2 zinc finger protein gene. *Plant Molecular Biology* **32**:785–796 DOI 10.1007/BF00020477.

Teif VB, Clarkson CT. 2019. Nucleosome positioning. In: *Encyclopedia of bioinformatics and computational biology*. Vol. 2. Amsterdam: Elsevier BV, 308–317 DOI 10.1016/B978-0-12-809633-8.20242-2.

Ueda M, Matsui A, Tanaka M, Nakamura T, Abe T, Sako K, Sasaki T, Kim JM, Ito A, Nishino N, Shimada H, Yoshida M, Seki M. 2017. The distinct roles of class I and II RPD3-like histone deacetylases in salinity stress response. *Plant Physiology* **175**:1760–1773 DOI 10.1104/pp.17.01332.

Varotto S, Locatelli S, Canova S, Pipal A, Motto M, Rossi V. 2003. Expression profile and cellular localization of maize Rpd3-type histone deacetylases during plant development. *Plant Physiology* **133**:606–617 DOI 10.1104/pp.103.025403.

Wang Z, Cao H, Chen F, Liu Y. 2014. The roles of histone acetylation in seed performance and plant development. *Plant Physiology and Biochemistry* **84**:125–133 DOI 10.1016/j.plaphy.2014.09.010.

Wolters H, Jurgens G. 2009. Survival of the flexible: hormonal growth control and adaptation in plant development. *Nature Reviews Genetics* **10**:305–317 DOI 10.1038/nrg2558.

Wu J, Zhang C, Mao P, Qian Y, Wang H. 2014. First report of leaf spot caused by *Nigrospora oryzae* on *Dendrobium candidum* in China. *Plant Disease* **98**:996–996 DOI 10.1094/PDIS-09-13-1006-PDN.

Wu K, Zhang L, Zhou C, Yu CW, Chaikam V. 2008. HDA6 is required for jasmonate response, senescence and flowering in *Arabidopsis*. *Journal of Experimental Botany* **59**:225–234 DOI 10.1093/jxb/erm300.

Xiong L, Schumaker KS, Zhu JK. 2002. Cell signaling during cold, drought, and salt stress. *The Plant Cell* **14**:S165–S183 DOI 10.1105/tpc.000596.

Yang C, Shen W, Chen H, Chu L, Xu Y, Zhou X, Liu C, Chen C, Zeng J, Liu J. 2018. Characterization and subcellular localization of histone deacetylases and their roles in response to abiotic stresses in soybean. *BMC Plant Biology* **18**:226 DOI 10.1186/s12870-018-1454-7.

Yang S, Zhang X, Cao Z, Zhao K, Wang S, Chen M, Hu X. 2014. Growth-promoting S phingomonas paucimobilis ZJSH 1 associated with *Dendrobium officinale* through phytohormone production and nitrogen fixation. *Microbial Biotechnology* **7**:611–620 DOI 10.1111/1751-7915.12148.

Yang X, Seto E. 2007. HATs and HDACs: from structure, function and regulation to novel strategies for therapy and prevention. *Oncogene* **26**:5310–5318 DOI 10.1038/sj.onc.1210599.

Zeng X, Ling H, Chen X, Guo S. 2019. Genome-wide identification, phylogeny and function analysis of GRAS gene family in *Dendrobium catenatum* (Orchidaceae). *Gene* **705**:5–15 DOI 10.1016/j.gene.2019.04.038.

Zhang GQ, Liu KW, Li Z, Lohaus R, Hsiao YY, Niu SC, Wang J-Y, Lin YC, Xu Q, Chen L-J. 2017. The *Apostasia* genome and the evolution of orchids. *Nature* **549**:379–383 DOI 10.1038/nature23897.

Zhang L, Eugeni EE, Parthun MR, Freitas MA. 2003. Identification of novel histone post-translational modifications by peptide mass fingerprinting. *Chromosoma* **112**:77–86 DOI 10.1007/S00412-003-0244-6.

Zhao L, Lu J, Zhang J, Wu PY, Yang S, Wu K. 2015. Identification and characterization of histone deacetylases in tomato (*Solanum lycopersicum*). *Frontiers in Plant Science* **5**:760 DOI 10.3389/fpls.2014.00760.

Zheng Y, Ge J, Bao C, Chang W, Liu J, Shao J, Liu X, Su L, Pan L, Zhou D-X. 2020. Histone deacetylase HDA9 and WRKY53 transcription factor are mutual antagonists in regulation of plant stress response. *Molecular Plant* **13**:598–611 DOI 10.1016/j.molp.2019.12.011.

Zhou C, Zhang L, Duan J, Miki B, Wu K. 2005. Histone deacetylase19 is involved in jasmonic acid and ethylene signaling of pathogen response in *Arabidopsis*. *The Plant Cell* **17**:1196–1204 DOI 10.1105/tpc.104.028514.